

CERN-TH/96-362
NORDITA 96/79-P
January 1997
hep-ph/9701309

Phenomenology of Power Corrections in Fragmentation Processes in e^+e^- Annihilation

M. BENEKE

*Theory Division, CERN,
CH-1211 Geneva 23, Switzerland*

V.M. BRAUN and L. MAGNEA *

NORDITA, Blegdamsvej 17, DK-2100 Copenhagen, Denmark

Abstract

We analyse power corrections to longitudinal and transverse fragmentation processes in e^+e^- annihilation, based on the assumption of ultraviolet dominance of power corrections. Under this assumption, we determine the dependence of power corrections on the scaling variable x from the infrared renormalon asymptotics of leading power coefficient functions. Our results suggest that the longitudinal and transverse gluon fragmentation coefficient functions receive corrections of order $1/(xQ)^2$. The power expansion breaks down at $x < \Lambda/Q$ and has to be resummed. This resummation leads to $1/Q$ corrections to the longitudinal and transverse cross section, which cancel for the total cross section. We provide a simple parametrization of the x dependence of $1/Q^2$ corrections to fragmentation processes and investigate perturbative corrections to the longitudinal cross section in higher orders, in view of a determination of the strong coupling.

*On leave of absence from Università di Torino, Torino, Italy.

1 Introduction

Inclusive single-particle production in e^+e^- collisions, $e^+e^- \rightarrow \gamma^*, Z^0 \rightarrow H(p) + X$, tests scaling violations in the time-like region and can be used to measure the strong coupling α_s [1, 2, 3]. Additional insight can be gained from a measurement of the angular dependence of the detected hadron [2, 3], since, for example, gluon fragmentation enters the longitudinal cross section as a leading contribution. The differential cross section can be expressed as [4]

$$\begin{aligned} \frac{d^2\sigma^H}{dx d\cos\theta}(e^+e^- \rightarrow HX) = & \frac{3}{8} (1 + \cos^2\theta) \frac{d\sigma_T^H}{dx}(x, Q^2) + \frac{3}{4} \sin^2\theta \frac{d\sigma_L^H}{dx}(x, Q^2) \\ & + \frac{3}{4} \cos\theta \frac{d\sigma_A^H}{dx}(x, Q^2). \end{aligned} \quad (1)$$

We defined $x = 2p \cdot q/q^2$, where p is the momentum of H and q the intermediate gauge boson momentum. $Q^2 = q^2$ denotes the center-of-mass energy squared and θ the angle between the hadron and the beam axis. The angular decomposition in (1) corresponds to the contributions from longitudinal and transverse polarizations of the intermediate gauge boson and from $\gamma^* - Z^0$ interference. In the following, we will not be concerned with the asymmetric contribution and with quark mass effects. Neglecting quark masses, $(1/\sigma_0) d\sigma_{T/L}^H/dx$ (where σ_0 is the Born total annihilation cross section) is independent of electroweak couplings and the longitudinal cross section is suppressed by α_s . The most precise measurements of fragmentation functions refer to a sum over all charged hadrons. In the following, we drop the superscript ‘ H ’ when a sum over all hadrons H is understood. The conversion from charged hadrons to all hadrons is considered as an ‘experimental problem’.

It follows from the factorization properties of perturbative QCD that the ‘structure functions’ in (1) are convolutions of perturbative coefficient functions $C_P^i(x, Q^2/\mu^2)$ ($P = T, L, A$) and parton fragmentation functions $D_i^H(x, \mu)$ ($i = q, \bar{q}, g$)¹,

$$\frac{d\sigma_P^H}{dx}(x, Q^2) = \sum_i \int_x^1 \frac{dz}{z} C_P^i(z, Q^2/\mu^2) D_i^H(x/z, \mu), \quad (2)$$

up to corrections suppressed by some power of Λ/Q , where Λ is the QCD scale parameter. The fragmentation functions have to be determined experimentally, but once measured, they can be used to predict fragmentation processes in other hard collisions. Both coefficient and fragmentation functions depend on the chosen factorization scheme and scale μ . We choose dimensional regularization with $\overline{\text{MS}}$ subtractions. Then the coefficient functions are obtained as the partonic cross sections with poles minimally subtracted. The fragmentation functions satisfy time-like evolution equations with kernels known to

¹For $i = q$ (or \bar{q}) we always imply that all light quark flavours are summed over. In the context of power corrections a quark is considered ‘light’ if its mass is smaller than Λ . Charm and bottom quarks must be treated separately, even if the center-of-mass energy is much larger than their masses.

next-to-leading order [5]. The coefficient functions in (2) have been computed to order α_s^2 [6].

The evolution kernels and perturbative corrections to coefficient functions cause scaling violations that are logarithmic in the center-of-mass energy. As in deep-inelastic scattering (DIS), multi-parton correlations, not taken into account in (2), lead to scaling violations that scale as some power of Λ/Q . Such corrections can nevertheless be important, as they can be enhanced in specific kinematic regions. Such a situation is well known for DIS, where for $x_{Bj} \rightarrow 1$ all partons must be highly correlated in order that all momentum can be transferred to a single parton. In this region, the twist expansion breaks down (see for example Ref. [7]). Unlike DIS, power corrections (in analogy with DIS we use ‘higher-twist correction’ synonymously) in fragmentation processes have rarely been studied theoretically [8]. The main difference comes from the applicability of the operator product expansion to DIS, which allows one to express the moments of multi-parton correlation functions [9] in terms of matrix elements of local operators. Such a classification seems to be more difficult for fragmentation, so that even the power behaviour of higher-twist corrections is not well established. Although the collinear (light-cone) expansion for fragmentation functions [8] is similar to that of structure functions in DIS and leads to the introduction of generalized multi-parton correlation functions for fragmentation that parametrize $1/Q^2$ corrections, the moments of these correlation functions remain non-local quantities and a separation of short and long distances is not straightforward. Phenomenological hadronization models are at variance with the light-cone expansion of Ref. [8], as they typically lead to $1/Q$ power corrections. The question of $1/Q$ versus $1/Q^2$ power behaviour is experimentally unsettled [3].

The second moment of single-particle inclusive cross sections summed over all hadrons is of particular interest. Because of the energy conservation sum rule

$$\sum_H \int_0^1 dx x D_i^H(x, \mu) = 1, \quad (3)$$

the fragmentation functions disappear from the integrals

$$\sigma_P \equiv \sum_H \frac{1}{2} \int_0^1 dx x \frac{d\sigma_P^H}{dx} = \sum_i \frac{1}{2} \int_0^1 dx x C_P^i(x), \quad (4)$$

which can therefore be calculated in perturbation theory up to corrections suppressed by some power of Λ/Q . The normalization is such that the total cross section $\sigma_{tot} = \sigma_L + \sigma_T$. For the longitudinal cross section [6]

$$\sigma_L = \sigma_0 \left[\frac{\alpha_s}{\pi} + (14.583 - 1.028N_f) \left(\frac{\alpha_s}{\pi} \right)^2 + \dots \right], \quad (5)$$

where $\alpha_s \equiv \alpha_s(Q)$ and N_f is the number of active fermion flavours. While dispersion relations relate the total cross section to the operator product expansion of a current correlation function, the power corrections to the longitudinal or transverse cross section

cannot be inferred from such methods. From the theoretical point of view, the longitudinal and transverse cross sections can be considered as event shapes, and little has been known about their power corrections until recently [10]–[16]. In Ref. [11] a $1/Q$ power correction to the longitudinal cross section was suggested as a consequence of phase-space reduction in the one-gluon emission diagram, when calculated with a massive gluon. At first sight, this conclusion seems to be again in conflict with the expectation [8] that fragmentation functions need to be corrected only at order $1/Q^2$.

The present paper is devoted to a theoretical analysis of power corrections in fragmentation processes.² We collect results of phenomenological character, which we hope can provide useful guidance in analysing fragmentation data collected at e^+e^- colliders and in extracting the strong coupling from the longitudinal cross section as well as, possibly, other event shape observables. The interpretation of our results in operator language [8] will be given in a subsequent paper.

In Sect. 2 we summarize the method, based on the infrared sensitivity of Feynman graphs, that allows us to estimate the x dependence of power corrections and clarify the assumptions that enter this approach. In Sect. 3, we give results for the power corrections to the quark and gluon coefficient functions. As will be explained, these power corrections factorize, so that the final estimate of power corrections to the fragmentation cross sections is given as a convolution with the leading twist fragmentation functions. A large part of Sect. 3 explores numerically the differences in various implementations of the method. Their comparison suggests an effective parametrization of $1/Q^2$ power corrections, presented in Sect. 3.5, which captures the gross features of the x dependence. This parametrization could be applied to LEP data [1, 2, 3], as a substitute for phenomenological hadronization corrections obtained from Monte Carlo programs. We also find that the power expansion is singular in the region where the detected hadron is soft and emanates from a gluon jet. For small values of x , the effective expansion parameter is $(\Lambda/(xQ))^2$. The consequences of these small- x singularities are pursued in Sect. 4, where we show that their resummation leads to a $1/Q$ power correction to the transverse and longitudinal cross section, thus resolving the apparent conflict with the light-cone expansion at fixed x . In Sect. 5 we argue that the large second-order correction in (5) is not accidental, but reflects the fact that the longitudinal cross section receives a $1/Q$ correction. This leads us to examine yet higher-order corrections in a certain approximation. We discuss their effect on a determination of α_s and the energy dependence of the longitudinal cross section with an eye on generic features that would equally apply to other event shape variables.

The results and conclusions of Sects. 3 and 4 overlap with those obtained independently by Dasgupta and Webber [18], who use a somewhat different model for the gluon contribution to the fragmentation functions. We discuss this difference and other ambiguities inherent in the method in Sect. 3.

² A preliminary account appeared in Ref. [17].

2 Method and assumptions

2.1 Ultraviolet dominance

Although the method we use to estimate the x dependence of higher-twist corrections has previously been used [19, 20, 21] in DIS, we find it useful to repeat the main ideas and to spell out the assumptions. Since the method applies without conceptual difference to fragmentation and DIS, it might be helpful to have DIS in mind as an example, for which the language of higher-twist corrections is familiar and higher-twist corrections can be interpreted within the operator product expansion.

We start from the observation that the separation of leading-twist from higher-twist is not unique. This is not apparent in low-order perturbative calculations in the $\overline{\text{MS}}$ scheme. Imagine, however, that the factorization in transverse momenta that is implicit in (2) were implemented by a rigid cut-off μ , such that only contributions from transverse momenta $k_t > \mu$ were included in the coefficient function C_P^i . Then one would find a term $\ln Q^2/\mu^2$, whose cut-off dependence is cancelled by the μ dependence of leading-twist fragmentation functions D_i^H , and in addition power-like cut-off dependence, starting with μ^2/Q^2 , which is cancelled by higher-twist contributions. Therefore the leading-twist contribution as a whole depends on the prescription used to implement the cut-off, just as the separation of leading-twist coefficient and fragmentation functions in (2) does. At first sight, such prescription dependence seems to be avoided in the $\overline{\text{MS}}$ scheme, because power-like dependence on the factorization scale μ does not exist. The problem reappears, however, because the coefficient function now has a factorially divergent series expansion in α_s (referred to as infrared renormalon divergence). Summing the series again requires a prescription and the prescription-dependence is power-suppressed precisely as the cut-off dependence above. In both cases, the ultraviolet renormalization of higher-twist operators must be performed consistently with the definition of the leading-twist coefficient function. The sum of leading-twist and higher-twist contributions is then unique. For the case at hand, setting $\mu = Q$ in (2), we can write the leading power ambiguity in the leading twist coefficient function as

$$\delta C_P^i(x) \propto A_{2,P}^i(x) \left(\frac{\Lambda}{Q} \right)^2 \quad (6)$$

times, possibly, logarithms of Λ/Q . The functions $A_{2,P}^i(x)$ are calculable in a certain approximation, as explained below.

Whichever point of view one prefers, there are two immediate conclusions: first, from the phenomenological point of view, higher-order contributions in perturbation theory and higher-twist corrections are inseparable and should be described by one parameter; second, precisely for this reason, some information on higher-twist effects can be obtained from the infrared (or large-order) behaviour of perturbation theory. If we could enumerate the higher-twist operators as in DIS, this piece of information would refer only to the ultraviolet regularization properties of these higher-twist operators, with an x dependence given by $A_{2,P}^i(x)$ in (6). In the following we will assume that the x de-

pendence of the entire higher-twist contribution is proportional to $A_{2,P}^i(x)$ and refer to this assumption as ‘ultraviolet dominance of higher-twist corrections’. Eq. (2) is then replaced by

$$\begin{aligned} \frac{d\sigma_P}{dx}(x, Q^2) = \sum_i \int_x^1 \frac{dz}{z} \left[C_P^i(z, Q^2/\mu^2) + K_2^i A_{2,P}^i(z) \frac{\Lambda^2}{Q^2} \right. \\ \left. + K_4^i A_{4,P}^i(z) \frac{\Lambda^4}{Q^4} + \dots \right] D_i(x/z, \mu). \end{aligned} \quad (7)$$

The dots denote higher power corrections and we anticipated that only even powers in $1/Q$ occur. The functions $A_{2,P}^i(z)$ will be given in Sect. 3.5 and the K_n^i are adjustable, z -independent constants that should be determined by comparison with experimental data. Note that here we slightly differ from previous formulations, where the constants are fixed in terms of an ‘effective coupling’ [19, 21] or equated to a universal constant [20] (fixed by the relation to the IR renormalon ambiguity). In our approach, these constants can depend on the factorization scale and also the order of perturbation theory to which the leading-twist coefficient function C_P^i has been calculated, since the added power corrections partly parametrize higher-order perturbative corrections as well. Naturally, the constants K_n^i should be ‘of order 1’. We emphasize again that for $i = q$, a sum over light quark flavours (u , d and s) is already included in $A_{n,P}^i(z)$.

Arguments related to infrared cut-off behaviour or infrared renormalons have been used repeatedly [16] to determine the scaling of power corrections with $1/Q$. In this case, no new information is obtained for DIS, where the power behaviour is known from the operator product expansion (OPE). The dependence of power corrections on x_{Bj} is not constrained by the OPE and is given in terms of multi-parton correlation functions, which are already too complex to be extracted from experiment. The ultraviolet dominance hypothesis provides tremendous simplifications, as the unknowns are reduced to a few constants rather than functions. Results that followed from applying this hypothesis to DIS structure functions have been found to reproduce experimental results on the x_{Bj} -dependence of higher-twist contributions unexpectedly well [19, 20, 21]. This empirical success encourages us to try the same idea for fragmentation processes.

The assumption that higher-twist corrections are proportional to their cut-off dependence (or renormalon ambiguity) does not become correct in any limit and therefore the resulting x dependence should be considered as a model. One should not insist on this proportionality too literally. Rather, the idea is that if the ultraviolet contribution to the higher-twist correction varies rapidly with x , one may expect that the full higher-twist correction also does, up to some smooth function. This expectation is best motivated by an analogy. Suppose we calculated some quantity to order α_s^n in perturbation theory. It is customary to vary the scale μ to get an idea about the size of the next term in the expansion. Of course, the μ -dependence gets exactly compensated, but if it is large (or small) the μ -independent terms are also expected to be large (or small). In the same way, although renormalon ambiguities are ultimately cancelled and unphysical, their x dependence should be indicative of the x dependence of the full higher-twist contribution.

Related to the choice of scale is the fact that in certain kinematical regions the scale of the hard process turns out to be of the form $\varepsilon(x)Q$, with $\varepsilon(x)$ typically given by a power of x or of $1-x$, because of phase-space restrictions for gluon emission. The physical scale is thus parametrically smaller than Q , and the power expansion is naturally organized in terms of $\Lambda/(\varepsilon(x)Q)$ rather than Λ/Q . Since kinematic restrictions affect large orders in perturbation theory, the ultraviolet behaviour of higher-twist operators and the entire higher-twist correction equally, the method outlined here will reproduce such parametric enhancements. Such enhancements will be seen to be crucial in understanding behaviour of power corrections to integrated fragmentation cross sections.

While the assumption of ultraviolet dominance of higher-twist corrections is definitively crude and clearly misses some features of higher-twist corrections (such as operators that do not mix into leading-twist ones through their ultraviolet behaviour), it should perhaps be measured by the simplicity with which some generic features of higher-twist corrections (and higher-order corrections in perturbation theory) can be incorporated.

2.2 Calculating $A_{n,P}^i(x)$

In this subsection we describe the calculation of the functions $A_{n,P}^i(x)$ in (7). They can be obtained either from lowest-order Feynman diagrams with an infrared regulator or from infrared renormalons in the large-order behaviour of the coefficient functions C_P^i . The precise form of $A_{n,P}^i(x)$ depends on the method chosen, although some equivalences can be found [22]. We adhere to the second method. In this case, the functions $A_{n,P}^i(x)$ are defined as the residues of IR renormalon poles of the Borel transform of C_P^i . This is still not practical, because it would require us to calculate the perturbative expansion of C_P^i to all orders. We therefore approximate the perturbative expansion by the series generated by inserting any number of fermion loops into the gluon line in diagrams that contribute at order α_s .

This class of diagrams falls into subclasses according to which parton is registered in the final state and where it originates from. Fig. 1 shows a contribution to the partonic cross section $d\sigma_P^q/dx$, where the registered quark originated at the primary virtual photon vertex. Another ‘primary’ quark contribution is obtained if, in Fig. 1, a gluon line instead of a fermion loop is cut. The registered quark can also come from a cut fermion loop. We refer to this contribution to $d\sigma_P^q/dx$, shown in Fig. 2, as ‘secondary’ quark contribution. Finally, the gluon cross section $d\sigma_P^g/dx$ is obtained from diagrams similar to that in Fig. 2, but with a cut gluon line instead of a fermion loop. In addition, diagrams with counterterm insertions have to be included. The antiquark cross section is identical to the quark cross section.

The set of diagrams with fermion loops is not really relevant by itself, as it typically yields small contributions to higher-order perturbative corrections. The main idea is to reinterpret the series in $(N_f\alpha_s)^n$ given by this set of diagrams as a series in $(\beta_0\alpha_s)^n$ and to restore the full QCD β -function coefficient $\beta_0 = -1/(4\pi)[11 - 2N_f/3]$ from the dependence on N_f ‘by hand’. This substitution seems difficult to justify, but comparison

with exact low-order results shows that it reproduces exact results quite well and that keeping corrections $(\beta_0\alpha_s)^n$ in higher orders resums important contributions. Further motivation can be found in [23, 24, 19].

The restoration of β_0 for the secondary quark contribution is especially delicate, since the fragmentation cross section depends on the ‘internal structure’ of the fermion loop, that is the phase-space over k_1 and k_2 (see Fig. 2) is non-trivially weighted. In such a situation, the association of fermion loops with running of the coupling is lost. To a certain extent, this intrinsic limitation of the method can be investigated by considering a fictitious theory with scalars rather than fermions in the fundamental representation. In this case we would compute scalar loop insertions and restore the full QCD β -function coefficient $\beta_0 = -1/(4\pi)[11 - N_s/6]$ from the dependence on N_s . We would like to obtain the same result as with fermions, since in both cases the important contributions are related to the non-abelian contribution to β_0 . For observables that resolve the internal structure of fermion or scalar loops, however, the resulting functions $A_{n,P}^i(x)$ are not identical. This difference leads to some model dependence, which is analysed in Sect. 3.

The fermion-loop approximation (and the massive gluon calculation, discussed in Sect. 2.3) also neglects multiple gluon emission. This is an obvious shortcoming of the method relevant at small values of x . The resummation of $\ln x$ contributions is crucial for particle multiplicities and the shape of fragmentation functions in the small- x region. In the following we consider the expansion in Q^2 at fixed x , leaving aside the question of the small- x asymptotics at fixed Q^2 . The order of limits is probably important. Renormalon and small- x resummations select different sets of diagrams and it is not known how to combine the two in a systematic way. See Sect. 4 for a further discussion of the problem. Related questions are also being discussed for Drell-Yan production [25, 26].

The evaluation of the two sets of diagrams shown in Fig. 1 and Fig. 2, for an arbitrary number of fermion-loop insertions, and for their sum, is straightforward by means of the dispersion technique discussed in Refs. [23, 24]. For a moment, let us consider only diagrams with a cut fermion bubble. It is convenient to organize the calculation such that the integral over the gluon virtuality (invariant mass of the $q\bar{q}$ pair) is done last. The main object of our interest will be the distribution in the gluon virtuality k^2 . To define it, consider for example the contribution of the diagrams in Fig. 1 or 2 to $d\sigma_P/dx$, summed over the number of fermion loops. It is given by³

$$\frac{d\sigma_P^{[p,s]}}{dx} = \int \frac{dk^2}{k^2} \frac{\beta_0^f \alpha_s}{|1 + \Pi(k^2)|^2} \frac{d\sigma_P^{[p,s]}}{dx} \left(x, \frac{k^2}{Q^2} \right), \quad (8)$$

where $\Pi(k^2)$ is the $\overline{\text{MS}}$ -renormalized fermion bubble, and the mass distribution can be written as

$$\frac{1}{\sigma_0} \frac{d\sigma_P^{[p,s]}}{dx}(x, \xi) \equiv \frac{8\pi}{N_c q^2} \int d\text{Lips}[p_1, p_2, k] (2\pi)^4 \delta^{(4)}(q - p_1 - p_2 - k) \frac{1}{k^2} \mathcal{M}_{\mu\nu} \mathcal{M}_{\mu'\nu'}^*$$

³The following equation should be considered as schematic, because the limit $k^2 \rightarrow 0$ needs some care. The correct treatment of this limit leads to (13) below. Alternatively, the equation can be understood as an expansion in α_s .

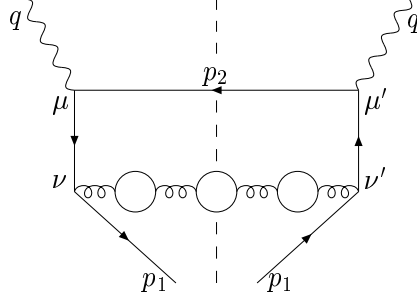


Figure 1: Example of a ‘primary’ quark contribution to the squared amplitude for $d\sigma_P^q/dx$. The set of all diagrams includes all attachments of the chain of fermion loops to the external quark line, the diagrams with a cut gluon line and an arbitrary number of fermion-loop insertions.

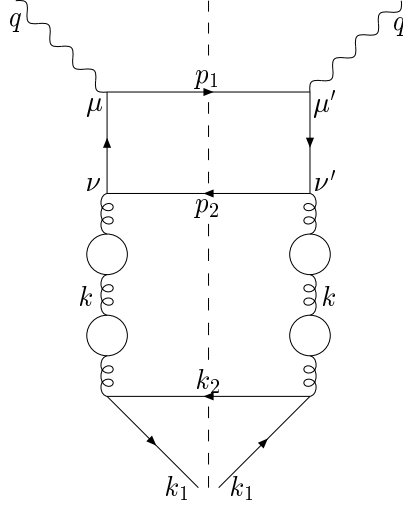


Figure 2: Example of a ‘secondary’ quark contribution to the squared amplitude for $d\sigma_P^q/dx$. The set of all diagrams includes all attachments of the chains of fermion loops to the external quark line and an arbitrary number of fermion-loop insertions.

$$\cdot \frac{2}{\beta_0^f} \int d\text{Lips}[k_1, k_2] (2\pi)^4 \delta^{(4)}(k - k_1 - k_2) \frac{N_f}{2} \text{Tr}[\gamma_\nu \not{k}_1 \gamma_{\nu'} \not{k}_2] \mathcal{P}_{P;\mu\mu'}^{[p,s]}(x) , \quad (9)$$

where $\xi = k^2/Q^2$. In Eq. (9), the notation for momenta and Lorentz indices corresponds to Fig. 2, and $\beta_0^f = N_f/(6\pi)$. We denote by $[p]$ ($[s]$) the ‘primary’ (‘secondary’) quark contribution, while $\int d\text{Lips}[\dots]$ are Lorentz-invariant phase-space integrals, and $\mathcal{M}_{\mu\nu}\mathcal{M}_{\mu'\nu'}^*$ is the matrix element for the primary $\gamma^* \rightarrow q\bar{q}g$ amplitude squared, divided by the square of the quark electric charge. The projections are such that (in the γ^* rest frame)

$$\mathcal{P}_{L+T;\mu\mu'}^{[s]}(x) = -\frac{g_{\mu\mu'}}{4} \delta\left(x - \frac{2k_1 q}{q^2}\right) , \quad (10)$$

$$\mathcal{P}_{L;\mu\mu'}^{[s]}(x) = \frac{k_{1,\mu}k_{1,\mu'}}{4|\vec{k}_1|^2} \delta\left(x - \frac{2k_1 q}{q^2}\right) , \quad (11)$$

for the secondary contribution to the total and longitudinal fragmentation function. For the longitudinal projection we used $q_\mu \mathcal{M}_{\mu\nu} = 0$, and the primary quark contribution is obtained by replacing k_1 with p_1 . The normalization factor $2/\beta_0^f$ in (9) may seem peculiar. It is chosen such that for inclusive quantities the distribution function coincides with the result that would be obtained from computing α_s -corrections with a massive gluon.

Note that in the case of the primary quark contribution the phase-space integral over k_1, k_2 is proportional to k^2 , so that the result takes the form of the one-loop diagram calculated with a gluon of mass k^2 . This ensures equivalence with the massive gluon calculation for this contribution. For the secondary quark contribution the projector depends on k_1 and modifies the phase-space integral. This is probably the simplest example of how event shapes in general are sensitive to the internal structure of fermion loops.

Given the invariant mass distributions in ξ , the contributions of fermion-loop diagrams to higher-order perturbative corrections are obtained in terms of the logarithmic moment integrals [23]

$$J_n(x) = \int_0^1 d\xi \ln^n \xi \frac{d}{d\xi} \frac{d\sigma_P^{[p,s]}}{dx}(x, \xi). \quad (12)$$

The sum of the series, defined by a principal value prescription for the Borel integral, equals

$$\frac{d\sigma_P^{(NNA)}}{dx} = \int_0^1 d\xi \Phi(\xi) \frac{d}{d\xi} \frac{d\sigma_P}{dx}(x, \xi) + \left[\frac{d\sigma_P}{dx}(x, \xi_L) - \frac{d\sigma_P}{dx}(x, 0) \right] , \quad (13)$$

where $\xi_L < 0$ is the position of the Landau pole in the strong coupling and the function $\Phi(\xi)$ is specified in Eq. (2.25) of the second reference in [23]. We shall make use of these results in Sect. 5.

To obtain the functions $A_{n,P}^i(x)$, it is not necessary to perform the final integration over k^2 (ξ). The infrared renormalon residues can be read off as coefficients of non-analytic terms in the expansion of the k^2 distribution $d\sigma_P/dx(x, \xi)$ at small ξ [22, 23]

$$\frac{d\sigma_P}{dx}(x, \xi) = \frac{d\sigma_P}{dx}(x, \xi \rightarrow 0) + \frac{C_F \alpha_s}{2\pi} \left\{ A_{1,P}(x) \sqrt{\xi} + A_{2,P}(x) \xi \ln \xi + A_{4,P}(x) \xi^2 \ln \xi + \dots \right\}. \quad (14)$$

Eq. (14) thus supplies all information required for the convolutions in (7).

Up to this point, we considered the partonic fragmentation cross sections $H = q, g$ in (2). To extract the coefficient functions C_P^i , the partonic fragmentation functions $D_i^{q,g}$ have to be calculated and subtracted in the same approximation. The need for subtractions is also reflected in the fact that the limit $\xi \rightarrow 0$ in (14) does not exist, because $d\sigma_P/dx \sim \ln \xi$ at small ξ . As a consequence, the integrals in (12) and (13) also diverge at small ξ . Once the partonic fragmentation functions are computed, the subtractions can be implemented into these equations by generalizing the case of ultraviolet subtractions discussed in [23] to infrared subtractions.

We emphasize that the power corrections added in (7) (that is the functions $A_{n,P}(x)$) depend on the factorization scheme and, for instance in the ‘annihilation scheme’, would differ from those in the $\overline{\text{MS}}$ -scheme, because the definition of the leading-twist fragmentation function can include an arbitrary set of power corrections. We will be working in the $\overline{\text{MS}}$ -scheme. In this particular scheme, we do not need to perform the subtractions explicitly and the functions $A_{n,P}(x)$ can already be obtained from the partonic cross sections. To see this, let us sketch how collinear factorization is performed for the set of diagrams considered above.

To solve (2) for C_P^i it is convenient to count powers of N_f for a given diagram, where N_f denotes the number of flavours. We expand the partonic fragmentation functions

$$D_i^k(x) = D_i^{k,[0]}(x) + \frac{1}{N_f} D_i^{k,[1]}(x) + \dots, \quad (15)$$

where $D_i^{k,[n]}(x)$ are power series in $N_f \alpha_s$. The leading order (in $1/N_f$) contributions are

$$D_q^{q,[0]}(x) = \delta(1-x), \quad (16)$$

$$D_g^{g,[0]}(x) = \delta(1-x) \frac{1}{1 - \beta_0^f \alpha_s / \epsilon}, \quad (17)$$

$$D_q^{g,[0]}(x) = 0, \quad (18)$$

$$D_g^{q,[0]}(x) = \frac{\alpha_s}{2\pi\epsilon} P_{g \rightarrow q}(x) + \mathcal{O}(N_f^2 \alpha_s^2), \quad (19)$$

where $P_{g \rightarrow q}(x) = N_f/2 [x^2 + (1-x)^2]$ denotes the DGLAP splitting function, $\beta_0^f = N_f/(6\pi)$ is the fermionic contribution to the β function, and $\epsilon = (4-d)/2$. Note that $D_g^{q,[0]}(x)$ contains an entire series in $N_f \alpha_s$, of which we show the first term only.

The factor $1/(1 - \beta_0^f \alpha_s/\epsilon)$ in $D_g^{g,[0]}(x)$ comes from counterterm insertions in fermion loops. Since the Born diagram leads to a non-vanishing coefficient function only for $C_T^q(x) = \delta(1-x)$, we find for the coefficient functions, in the fermion-loop approximation,

$$C_L^g(x) = \left(1 - \frac{\beta_0^f \alpha_s}{\epsilon}\right) \frac{d\sigma_L^g}{dx} = \frac{C_F \alpha_s}{2\pi} \frac{4(1-x)}{x}, \quad (20)$$

$$C_L^q(x) = \frac{d\sigma_L^q}{dx} - C_L^g * D_g^{q,[0]}, \quad (21)$$

$$C_T^g(x) = \left(1 - \frac{\beta_0^f \alpha_s}{\epsilon}\right) \left(\frac{d\sigma_T^g}{dx} - D_q^{g,[1]}\right), \quad (22)$$

$$C_T^q(x) = \frac{d\sigma_T^q}{dx} - D_q^{q,[1]} - C_T^g * D_q^{q,[0]}. \quad (23)$$

The asterisk denotes convolution. The coefficient functions have finite limits as $\epsilon \rightarrow 0$. Note that in the fermion-loop approximation, the longitudinal gluon coefficient function has no corrections beyond first order. The graphs with uncut fermion loops are cancelled by analogous contributions to D_g^g . On the other hand, the longitudinal quark coefficient function and the transverse coefficient functions involve non-trivial subtractions.

However, as long as we are interested only in power corrections (infrared renormalons) and not in the complete higher-order perturbative corrections, we do not need to calculate these subtractions explicitly. The partonic fragmentation functions needed in our approximation have convergent series expansions and do not contribute to infrared renormalon residues. This property is specific to minimal subtraction schemes, where partonic fragmentation functions are expressed as pure poles in ϵ . For the ξ distributions introduced above, this implies that the $\ln \xi$ terms are removed, but all other non-analytic terms, and in particular the functions $A_P^i(x)$, remain unaltered by factorizing the fragmentation functions.

It is important that the mixing between quark and gluon operators at leading twist repeats itself at the level of power corrections and renormalons. Although the gluon coefficient functions are convergent series in the fermion-loop approximation, this does not mean that gluon fragmentation does not give rise to power corrections. Because of mixing, the infrared renormalons in quark coefficient functions due to the secondary quark contribution are cancelled by ultraviolet renormalons in quark matrix elements of gluon operators of higher twist. The same gluon operators also have non-vanishing gluon matrix elements, which are set to zero only in the formal large- N_f limit.

2.3 Massive gluon scheme

It can be shown [22, 23] that for sufficiently inclusive observables, the functions $A_{n,P}^i(x)$ obtained from the residues of IR renormalons in the above approximation to the perturbative series can also be obtained from the α_s corrections alone, provided they are

computed with non-vanishing gluon mass. In this case, these functions can be read off from non-analytic terms in the small-mass expansion.⁴ This equivalence does not hold for general event shapes, which are sensitive to the internal structure of fermion loops, as is the case for the secondary quark contribution in Fig. 2 (and as discussed in Ref. [14]).

Although in this situation a formal justification of the massive gluon scheme is lacking, except, perhaps, as an ad hoc implementation of the general idea of scale separation by an explicit infrared cut-off, we find it useful to check whether the massive gluon calculation reproduces the gross features of the fermion-loop calculation. If so, one could take advantage of the relative simplicity of the massive gluon calculation.

With this motivation in mind, we will present also the distribution functions in ξ in the massive gluon scheme (see also [18]). We will find that the comparison between the fermion loop and massive gluon calculation has to be done case by case, with varying conclusions.

2.4 Summary of distribution functions

In this subsection we present our results for the distributions in ξ corresponding to the detection of the primary and the secondary quark, as well as those corresponding to the detection of a gluon, calculated in the massive gluon scheme. We give the exact expressions, as well as the small- ξ expansions corresponding to (14), and we extract the coefficients $A_{j,p}^i(x)$ of the power corrections. As explained above, the gluon coefficient function is trivial in the large-order approximation we have adopted and does not indicate power corrections. The role of the gluon coefficient is taken by the secondary quark contribution, Fig. 2, to the quark coefficient function. The results presented below refer to the sum of quark and antiquark contributions, which amounts to multiplying the quark contribution by two.

2.4.1 Primary quark contribution

For the primary quark contribution to $d\sigma_P^q/dx$ (Fig. 1), the distribution in k^2 coincides with the partonic quark fragmentation cross section calculated with a massive gluon. Defining $\xi = k^2/Q^2$ as before we have

$$\begin{aligned} \frac{1}{\sigma_0} \frac{d\sigma_L^{q,[p]}}{dx} &= \frac{C_F \alpha_s}{2\pi} \cdot 2 \cdot \Theta(1 - \xi - x) \left[1 + \xi \left(\frac{6}{x} - 2 - \frac{2}{1-x} \right) + \xi^2 \left(-\frac{6}{x} - \frac{4}{1-x} \right. \right. \\ &\quad \left. \left. + \frac{1}{(1-x)^2} \right) + \frac{2\xi}{x^2} (2x + 3\xi) \ln \frac{\xi}{(1-x)(x+\xi)} \right], \end{aligned} \quad (24)$$

$$\frac{1}{\sigma_0} \frac{d\sigma_T^{q,[p]}}{dx} = \frac{C_F \alpha_s}{2\pi} \cdot 2 \cdot \left\{ \delta(1-x) \left[2(1+\xi)^2 \left(\text{Li}_2(-\xi) - \frac{1}{2} \ln^2 \xi + \ln \xi \ln(1+\xi) + \frac{\pi^2}{6} \right) \right. \right.$$

⁴The restriction to non-analytic terms is clear. Analytic terms in λ^2 also arise from large k^2 , where the propagator $1/(k^2 + \lambda^2)$ can be Taylor-expanded in λ^2 .

$$\begin{aligned}
& - (3 + 2\xi) \ln \xi - \frac{7}{2} - 2\xi \Big] + \Theta(1 - \xi - x) \Big[- \frac{3 - 5\xi^2}{2(1 - x)} + \frac{\xi}{(1 - x)^2} \\
& + \frac{\xi^2}{2(1 - x)^3} + \frac{\xi}{x + \xi} - \frac{6\xi(1 - \xi)}{x} - \frac{1 - x}{2} + 3\xi \\
& - \left(\frac{2(1 + \xi)^2}{1 - x} - 1 - x - 2\xi + \frac{4\xi}{x} + \frac{6\xi^2}{x^2} \right) \ln \frac{\xi}{(1 - x)(x + \xi)} \Big] \Big\}. \tag{25}
\end{aligned}$$

The expansion in ξ gives

$$\begin{aligned}
\frac{1}{\sigma_0} \frac{d\sigma_L^{q,[p]}}{dx} &= \frac{C_F \alpha_s}{2\pi} \cdot 2 \cdot \left[1 + \xi \ln \xi A_{2,L}^{q,[p]}(x) + \xi \left(\frac{6}{x} - 2 - \frac{2}{[1 - x]_+} + \frac{4}{x} \ln \frac{1}{x(1 - x)} \right) \right. \\
& \left. + \xi^2 \ln \xi A_{4,L}^{q,[p]}(x) + O(\xi^2) \right], \tag{26}
\end{aligned}$$

where

$$A_{2,L}^{q,[p]}(x) = 2\delta(1 - x) + \frac{4}{x}, \tag{27}$$

$$A_{4,L}^{q,[p]}(x) = \delta'(1 - x) + 4\delta(1 - x) + \frac{6}{x^2}. \tag{28}$$

The δ functions arise from expanding singular functions around the phase-space boundary $1 - x - \xi$. For the transverse cross section, we keep only non-analytic terms in the expansion; then

$$\begin{aligned}
\frac{1}{\sigma_0} \frac{d\sigma_T^q}{dx} &= \frac{C_F \alpha_s}{2\pi} \cdot 2 \cdot \left[- \ln \xi \left(\frac{1 + x^2}{[1 - x]_+} + \frac{3}{2} \delta(1 - x) \right) + \xi \ln \xi A_{2,T}^{q,[p]}(x) \right. \\
& \left. + \xi^2 \ln \xi A_{4,T}^{q,[p]}(x) + O(\xi^3 \ln \xi) \right], \tag{29}
\end{aligned}$$

where

$$A_{2,T}^{q,[p]}(x) = - \frac{4}{[1 - x]_+} + 2 - \frac{4}{x} - 2\delta(1 - x) + \delta'(1 - x), \tag{30}$$

$$A_{4,T}^{q,[p]}(x) = - \frac{2}{[1 - x]_+} - \frac{6}{x^2} - \frac{5}{2} \delta(1 - x) - \frac{1}{4} \delta''(1 - x). \tag{31}$$

2.4.2 Secondary quark contribution

Because of cancellations between the longitudinal and transverse cross sections it is more convenient to quote the distribution in ξ for the longitudinal contribution and the sum

of transverse and longitudinal contributions,

$$\begin{aligned}
\frac{1}{\sigma_0} \frac{d\sigma_L^{q,[s]}}{dx} = & \frac{C_F \alpha_s}{2\pi} \cdot 2 \cdot \Theta(1-x) \Theta(x-\xi) \left[-\frac{15\xi(1+\xi)}{8x^2} \right. \\
& + \frac{3(1-\xi)(5\xi^2 + 10\xi x^2 - 3x^4)}{16\xi x^2} \ln \xi - 6\frac{\xi}{x} \ln x \ln \frac{x}{\xi} \\
& + \frac{3}{8\xi x} (5\xi + 2\xi^2 + 5\xi^3 + 6\xi x + 6\xi^2 x - 3x^2 - 14\xi x^2 - 3\xi^2 x^2 + 3x^3 + 3\xi x^3) \\
& + \frac{3}{16\xi x} (5\xi + 18\xi^2 + 5\xi^3 - 16\xi x - 16\xi^2 x + 3x^2 - 2\xi x^2 + 3\xi^2 x^2) \ln \frac{\xi}{x^2} \\
& - \frac{3}{8\xi x^2} (5\xi^2 + 18\xi^3 + 5\xi^4 - 6\xi x^2 + 4\xi^2 x^2 - 6\xi^3 x^2 - 3x^4 + 2\xi x^4 \\
& \left. - 3\xi^2 x^4) T(\sqrt{\xi}, x) \right], \tag{32}
\end{aligned}$$

$$\begin{aligned}
\frac{1}{\sigma_0} \frac{d\sigma_{L+T}^{q,[s]}}{dx} = & \frac{C_F \alpha_s}{2\pi} \cdot 2 \cdot \Theta(1-x) \Theta(x-\xi) \left[\frac{36(1+\xi)}{x^2} \right. \\
& - \frac{12}{\xi x^3} (4\xi^2 - x^2 + 2\xi x^2 - \xi^2 x^2 + x^3 + \xi x^3) + \frac{6(1-\xi)}{\xi x^2} (x^2 + 3\xi) \ln \xi \\
& - \frac{6}{\xi x^3} (-2\xi^2 - 2\xi x - 2\xi^2 x + x^2 + 4\xi x^2 + \xi^2 x^2) \ln \frac{\xi}{x^2} \\
& \left. - \frac{24(1+x+\xi)}{x^2} \ln x \ln \frac{x}{\xi} - \frac{12}{\xi x^2} (1+\xi)^2 (x^2 + 3\xi) T(\sqrt{\xi}, x) \right], \tag{33}
\end{aligned}$$

where

$$\begin{aligned}
T(\lambda, x) \equiv & \int_{1/x}^1 dt \frac{\ln(\lambda t)}{1 + \lambda^2 t^2} = \frac{i}{2\lambda} \left[\ln \lambda \ln \frac{1-i\lambda}{1+i\lambda} - \ln \frac{\lambda}{x} \ln \frac{x-i\lambda}{x+i\lambda} \right. \\
& \left. + \text{Li}_2(i\lambda) - \text{Li}_2(-i\lambda) - \left(\text{Li}_2\left(i\frac{\lambda}{x}\right) - \text{Li}_2\left(-i\frac{\lambda}{x}\right) \right) \right]. \tag{34}
\end{aligned}$$

The $\xi \rightarrow 0$ limits and the first non-analytic terms in the expansion at small ξ are given by

$$\frac{1}{\sigma_0} \frac{d\sigma_L^{q,[s]}}{dx} = \frac{C_F \alpha_s}{2\pi} \cdot 2 \cdot \left[\frac{4}{x} - 6x + 2x^2 + 6 \ln x + \xi \ln \xi A_{2,L}^{q,[s]}(x) \right]$$

$$+\xi^2 \ln \xi A_{4,L}^{q,[s]}(x) + \dots \Big], \quad (35)$$

$$\begin{aligned} \frac{1}{\sigma_0} \frac{d\sigma_{L+T}^{q,[s]}}{dx} = \frac{C_F \alpha_s}{2\pi} \cdot 2 \cdot \Bigg[& -\ln \xi \left(2 \cdot \frac{3}{N_f} \cdot \frac{1}{C_F} \cdot [P_{q \rightarrow g} * P_{g \rightarrow q}](x) \right) + \xi \ln \xi A_{2,L+T}^{q,[s]}(x) \\ & + \xi^2 \ln \xi A_{4,L+T}^{q,[s]}(x) + \dots \Bigg], \end{aligned} \quad (36)$$

where

$$A_{2,L}^{q,[s]}(x) = \frac{6}{5x^3} + \frac{4}{x} - 6 + \frac{4}{5}x^2 + \frac{6 \ln x}{x}, \quad (37)$$

$$A_{4,L}^{q,[s]}(x) = -\frac{16}{35x^5} + \frac{16}{5x^3} - \frac{4}{x^2} + \frac{8}{5} - \frac{12}{35}x^2, \quad (38)$$

$$A_{2,L+T}^{q,[s]}(x) = \frac{6}{5x^3} - \frac{11}{x} + 9 + \frac{4}{5}x^2 - 6 \ln x, \quad (39)$$

$$A_{4,L+T}^{q,[s]}(x) = -\frac{24}{35x^5} + \frac{12}{5x^3} - \frac{4}{x} + \frac{12}{5} - \frac{4}{35}x^2. \quad (40)$$

Note that the expansions in ξ are valid only for $x > \sqrt{\xi}$, although x can be as small as ξ . The minimal invariant mass of the $q\bar{q}$ pair, however, is attained at $x = \sqrt{\xi}$.

The $\xi \rightarrow 0$ limits in (35) and (36) require explanation. First note that although the diagrams in Fig. 1 and Fig. 2 start at order α_s^2 , our resulting distribution functions are written as order α_s . Technically, this can be best understood by considering the Borel transform of the series generated by these diagrams. Since there is no diagram at order α_s , one would expect the Borel transform to vanish linearly in u , the Borel parameter, at small u . However, the $g \rightarrow q\bar{q}$ splitting amplitude contains a collinear divergence, which manifests itself as a pole $1/u$. Consequently, the Borel transform approaches a constant for small u , which corresponds to an α_s contribution. The collinear pole in u indicates that collinear subtractions need to be performed. Indeed, if $C_L^g * D_g^{q,[0]}$ is subtracted as required by (21), the constant term in the Borel transform vanishes and the secondary quark contribution to the quark coefficient function is of order α_s^2 , as it should be.

To check this cancellation, we observe that the leading term in (35) can be rewritten as

$$\frac{C_F \alpha_s}{2\pi} \cdot 2 \cdot \left[\frac{4}{x} - 6x + 2x^2 + 6 \ln x \right] = 2 \cdot \frac{3}{N_f} \cdot [C_L^g * P_{g \rightarrow q}](x), \quad (41)$$

with C_L^g defined in (20). As expected from the above discussion, the $\xi \rightarrow 0$ limit of the secondary quark contribution is just the gluon coefficient function convoluted with collinear splitting into a $q\bar{q}$ pair. The factor 2 accounts for the sum over quark and antiquarks. The factor $3/N_f$ is the large- N_f limit of $\alpha_s/(2\pi) \cdot \ln Q^2/\Lambda^2$ associated with the $g \rightarrow q\bar{q}$ amplitude.

The $\ln \xi$ term in the sum of the longitudinal and transverse cross sections can likewise be interpreted as a convolution of two subsequent $q(\bar{q}) \rightarrow g$ and $g \rightarrow q(\bar{q})$ splittings, as indicated in (36).

We should stress again that these complications associated with collinear factorization do not affect the non-analytic terms in the expansion in ξ , except for $\ln \xi$, and therefore do not affect the expressions for $A_{n,P}^i$. Note that for heavy quark fragmentation, the secondary quark contribution would not give rise to power corrections, because the invariant mass distribution is cut off at $4m_Q^2$.

2.4.3 Massive gluon scheme

For completeness and later comparison, we quote the distribution functions in the massive gluon scheme. The distribution functions are given as the partonic fragmentation cross sections to order α_s , computed with a massive gluon. The quark fragmentation cross sections are identical to our primary quark contributions, Sect. 3.1.1. The gluon cross sections read

$$\frac{1}{\sigma_0} \frac{d\sigma_L^{g,\text{MG}}}{dx} = \frac{C_F \alpha_s}{2\pi} \Theta(1 + \xi - x) \Theta(x - 2\sqrt{\xi}) \cdot 4(1 + \xi) \frac{1 + \xi - x}{\sqrt{x^2 - 4\xi}} \left[1 - \frac{2\xi}{x} \frac{1}{\sqrt{x^2 - 4\xi}} \ln \frac{(x + \sqrt{x^2 - 4\xi})^2}{4\xi} \right], \quad (42)$$

$$\begin{aligned} \frac{1}{\sigma_0} \frac{d\sigma_{L+T}^{g,\text{MG}}}{dx} &= \frac{C_F \alpha_s}{2\pi} \Theta(1 + \xi - x) \Theta(x - 2\sqrt{\xi}) \left[-4\sqrt{x^2 - 4\xi} \right. \\ &\quad \left. + \frac{2}{x} [2(1 + \xi)(1 + \xi - x) + x^2] \ln \frac{(x + \sqrt{x^2 - 4\xi})^2}{4\xi} \right]. \end{aligned} \quad (43)$$

As $\xi \rightarrow 0$, the longitudinal cross section reduces to (20). Expansion in ξ results in

$$\frac{1}{\sigma_0} \frac{d\sigma_L^{g,\text{GM}}}{dx} = \frac{C_F \alpha_s}{2\pi} \left[\frac{4(1-x)}{x} + \xi \ln \xi A_{2,L}^{g,\text{MG}}(x) + \xi^2 \ln \xi A_{4,L}^{g,\text{MG}}(x) + \dots \right] \quad (44)$$

$$\begin{aligned} \frac{1}{\sigma_0} \frac{d\sigma_{L+T}^{g,\text{GM}}}{dx} &= \frac{C_F \alpha_s}{2\pi} \left[-2 \cdot \ln \xi \frac{(1 + (1-x)^2)}{x} + \xi \ln \xi A_{2,L+T}^{g,\text{MG}}(x) \right. \\ &\quad \left. + \xi^2 \ln \xi A_{4,L+T}^{g,\text{MG}}(x) + \dots \right], \end{aligned} \quad (45)$$

where again we have kept only the leading term and the first few non-analytic terms. The coefficients of power corrections are now given by

$$A_{2,L}^{g,\text{MG}}(x) = \frac{8(1-x)}{x^3}, \quad (46)$$

$$A_{4,L}^{g,\text{MG}}(x) = \frac{8(2-x)}{x^3} + \frac{32(1-x)}{x^5} , \quad (47)$$

$$A_{2,L+T}^{g,\text{MG}}(x) = -\frac{8}{x} + 4 - 2\delta(1-x) , \quad (48)$$

$$A_{4,L+T}^{g,\text{MG}}(x) = -\frac{4}{x} - 3\delta(1-x) - \delta'(1-x) . \quad (49)$$

Our results in the massive gluon scheme coincide with those obtained by Dasgupta and Webber [18].

3 Power corrections to fragmentation functions

In this section we analyse the x dependence of power corrections. We present predictions in the fermion-loop approximation and then discuss in detail the ambiguities related to the restoration of the gluon fragmentation component. To this end, we compare the fermion-loop calculation with the massive gluon calculation and check the effect of replacing fermions by scalars. Once again, ‘massive gluon calculation’ refers to the identification of power corrections through non-analytic contributions in the expansion of order- α_s corrections in a small gluon mass, as done in Ref. [18]. Finally, in Sect. 3.5, we abstract from the discussion the generic dependences on x and formulate a simple phenomenological parametrization of $1/Q^2$ corrections consistent with our results.

3.1 Results

To illustrate the magnitude of the leading $1/Q^2$ power corrections to the fragmentation cross sections in e^+e^- annihilation in the fermion-loop approximation, we rewrite (7) as

$$\frac{d\sigma_P}{dx}(x, Q^2) = F_P(x, Q^2) \left[1 + H_{2,P}(x, Q^2) \frac{\Lambda^2}{Q^2} + \dots \right] , \quad (50)$$

where

$$F_P(x, Q^2) = \sum_i \left[C_P^i * D_i \right] (x, Q^2) = \sum_i \int_x^1 \frac{dz}{z} C_P^i(z, Q^2/\mu^2) D_i(x/z, \mu) \quad (51)$$

denotes the leading-twist cross section. The power correction is given by

$$H_{2,P}(x, Q^2) \equiv \sum_i K_2^i \frac{\left[A_{2,P}^i * D_i \right] (x, Q^2)}{F_P(x, Q^2)} = \frac{1}{F_P(x, Q^2)} \sum_i \int_x^1 \frac{dz}{z} K_2^i A_{2,P}^i(z) D_i(x/z, \mu). \quad (52)$$

In the following, we set $K_2^q = 1$. Since in the fermion-loop approximation we only have a quark (antiquark) contribution, no information is lost, as the over-all scale is then set by Λ^2 in (50). We use the ALEPH parametrization [3] of the (light) quark (and later,

gluon) fragmentation function at $Q = \sqrt{s} = 22 \text{ GeV}$ and their value $\alpha_s(22\text{GeV}) = 0.164$. In evaluating $F_P(x, Q^2)$, we use the lowest-order approximation to the leading-twist coefficient function C_P^q .

The result for $H_{2,P}(x)$ for the longitudinal and transverse fragmentation cross sections, summed over all hadrons, as a function of energy fraction x is shown in Figs. 3 and 4, respectively. The sum of longitudinal and transverse cross sections, which differs from the total cross section by the small asymmetric contribution due to γ/Z^0 interference, is shown in Fig. 5. We recall that $F_L/F_T \sim \alpha_s$, so that the relative magnitude of power corrections is enhanced for longitudinal fragmentation as reflected by the scales on the vertical axes in Fig. 3 and 4. We note that for $x > 0.2$ the power correction to both, longitudinal and transverse, cross sections is dominated by primary quark fragmentation. Such a qualitative behaviour is expected, since the average energy of a quark connected to the ‘hard’ γ^* or Z^0 vertex is much larger than the average energy of a quark originating from gluon splitting. Since for the primary quark contribution the restoration of β_0 from the dependence on N_f is unproblematic and the fermion-loop and massive gluon calculations coincide, the method yields an unambiguous prediction at $x > 0.2$. At smaller values of x the secondary quark contribution becomes important for the longitudinal cross section and for the sum of longitudinal and transverse cross sections, but remains small for the transverse one. Comparing Figs. 3–5 with the corresponding figures in Ref. [18], obtained from the massive gluon calculation, one concludes that the results are qualitatively similar for the longitudinal cross section, but differ drastically at small x for the others. The difference can be traced to the absence of a $1/x^3$ term in $A_{2,L+T}^{g,\text{MG}}(x)$, Eq. (48), as compared to $A_{2,L+T}^{q,[s]}(x)$, Eq. (39), and will be discussed in detail in Sect. 3.4.

Let us comment on the normalization of $H_{2,P}(x)$. With $K_2^i = 1$, the overall normalization of $A_{2,P}$ was obtained by setting $C_F\alpha_s/(2\pi)\xi \ln \xi \rightarrow \Lambda^2/Q^2$ in the distribution functions. If we took the normalization literally from the IR renormalon ambiguity of the Borel integral, divided by π , we would have to substitute

$$\frac{C_F\alpha_s}{2\pi}\xi \ln \xi \rightarrow \frac{C_F e^{5/3}}{2\pi(-\beta_0)} \frac{\Lambda^2}{Q^2} \approx 1.6 \frac{\Lambda^2}{Q^2}, \quad (53)$$

where $\Lambda = Q \exp(1/(2\beta_0\alpha_s(Q)))$. With this substitution, using α_s as given above and $H_{2,L+T}(x) \sim 15$ for intermediate x , the power correction in Fig. 5 scales as $(0.7 \text{ GeV}/Q)^2$, very similar in magnitude to what is obtained with an ‘effective coupling’ [18]. For phenomenological analyses we suggest that the overall normalization be fitted to the data.

3.2 Restoring gluons

In the above analysis, all power corrections are obtained as convolution with the quark fragmentation function. But the original motivation was to compute fermion loops only to trace the dominating non-abelian (gluon) contribution through the dependence on

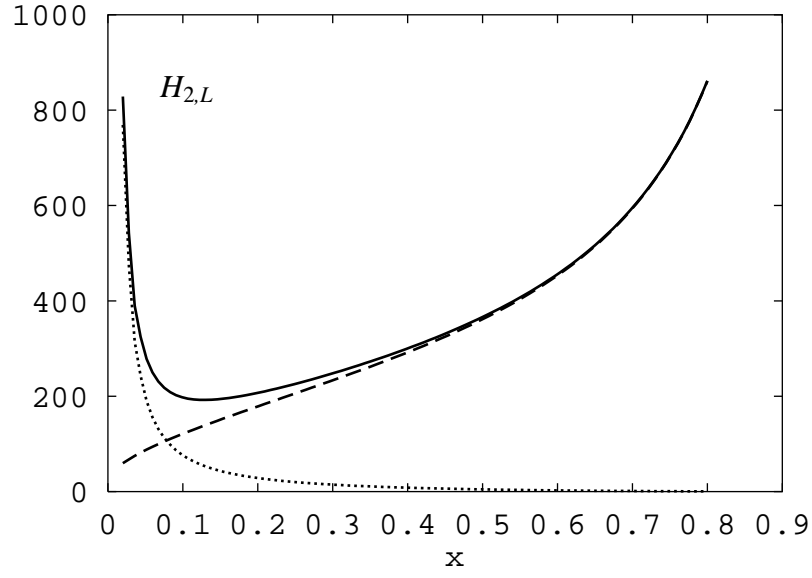


Figure 3: Shape of $1/Q^2$ power correction $H_{2,L}(x)$ to the longitudinal fragmentation cross section. Dashed line: primary quark contribution. Dotted Line: secondary quark contribution. Solid line: sum of both.

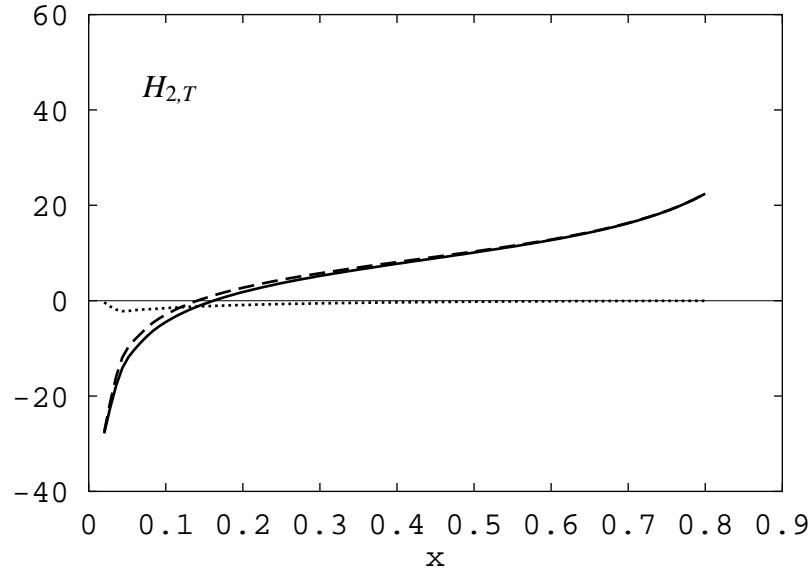


Figure 4: Shape of $1/Q^2$ power correction $H_{2,T}(x)$ to the transverse fragmentation cross section. Dashed line: primary quark contribution. Dotted Line: secondary quark contribution. Solid line: sum of both.

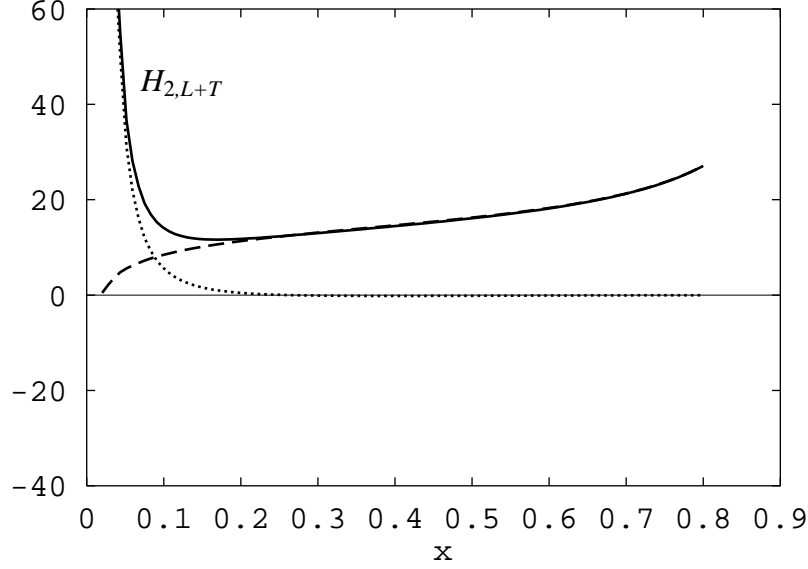


Figure 5: Shape of $1/Q^2$ power correction $H_{2,L+T}(x)$ to the sum of longitudinal and transverse fragmentation cross sections. Dashed line: primary quark contribution. Dotted Line: secondary quark contribution. Solid line: sum of both.

N_f . Eventually, the secondary quark contribution should therefore be reinterpreted as a gluon fragmentation contribution.

Such a reinterpretation faces ambiguities, and we would like to single out the gross features, which can be considered as unique. To have a basis for comparison, we first ‘deconvolute’ the $g \rightarrow q\bar{q}$ splitting from the secondary quark contribution. We define the ‘effective gluon’ coefficient functions $A_{2,P}^{g \leftarrow q}(x)$ through

$$\left[A_{2,P}^{g \leftarrow q} * P_{g \rightarrow q} \right] (x) = A_{2,P}^{q,[s]}(x), \quad (54)$$

which should be convoluted with the gluon fragmentation function, replacing $A_{2,P}^{q,[s]}$ convoluted with the quark fragmentation function. The superscript $g \leftarrow q$ indicates that the present effective gluon coefficient has been obtained by deconvoluting a quark emission amplitude. Below we will consider an analogous coefficient obtained from a scalar quark emission amplitude. Although

$$A_{2,P}^{g \leftarrow q} * D_g = A_{2,P}^{q,[s]} * D_q \quad (55)$$

holds only to leading logarithmic accuracy in Q^2 , this is the closest one can get to reinterpreting the secondary quark contribution as a gluon contribution. The functions $A_{2,P}^{g \leftarrow q}(x)$ can be compared directly with the $A_{2,P}^{g,\text{MG}}(x)$ obtained in the massive gluon calculation.

To test the sensitivity of the deconvolution to the particular structure of the quark-gluon vertex, we compute $A_{n,P}$ in a (fictitious) theory with scalar particles rather than

fermions (quarks). Then we deconvolute the gluon-scalar splitting function $P_{g \rightarrow sq}(x) = x(1-x)/2$ to obtain the effective gluon coefficient $A_{2,P}^{g \leftarrow sq}(x)$. The gluon interpretation of the secondary quark contribution is justified only if this function, after convolution with the gluon fragmentation function, leads to results compatible with those obtained starting from quarks.

To obtain the functions $A_{n,P}$ for scalars, one replaces (neglecting terms that vanish when contracted with $\mathcal{M}_{\mu\nu}$) the trace

$$\frac{2}{\beta_0^f} \cdot \frac{N_f}{2} \text{Tr}[\gamma_\nu \not{k}_1 \gamma_{\nu'} \not{k}_2] = 6\pi \left(-8k_{1\nu}k_{1\nu'} - 2k^2 g_{\nu\nu'} \right) \quad (56)$$

in (9) by

$$\frac{2}{\beta_0^{sf}} \cdot \frac{N_s}{2} (k_1 - k_2)_\nu (k_1 - k_2)_{\nu'} = 24\pi \cdot 4k_{1\nu}k_{1\nu'}. \quad (57)$$

When the phase-space over k_1 and k_2 is integrated unweighted, the integrals of the previous two equations coincide. Because of the projection $\mathcal{P}_{P;\mu\mu'}^{[s]}$ in (9), however, Eqs. (37)–(40) for the secondary quark contribution are replaced by

$$A_{2,L}^{sq,[s]}(x) = \frac{2}{5x^3} - \frac{2}{x} + 2 - \frac{2}{5}x^2, \quad (58)$$

$$A_{4,L}^{sq,[s]}(x) = -\frac{6}{35x^5} + \frac{2}{5x^3} - \frac{2}{5} + \frac{6}{35}x^2, \quad (59)$$

$$A_{2,L+T}^{sq,[s]}(x) = \frac{2}{5x^3} - \frac{2}{x} + 2 - \frac{2}{5}x^2, \quad (60)$$

$$A_{4,L+T}^{sq,[s]}(x) = -\frac{9}{35x^5} + \frac{4}{5x^3} - \frac{1}{x} + \frac{2}{5} + \frac{2}{35}x^2, \quad (61)$$

for scalar particles. Note that $A_{2,T}^{sq,[s]}(x) = 0$.

For the interesting case of a gluon splitting into two gluons, the expression replacing (56) is still a linear combination of only two Lorentz structures $k_{1,\nu}k_{1,\nu'}$ and $k^2 g_{\nu\nu'}$. Therefore all ambiguities related to restoring β_0 are already exhausted by a linear combination of the results obtained for fermions and for scalars. In particular, if one computes the graphs with one cut gluon loop in an axial gauge, the coefficient of $k_{1\nu}k_{1\nu'}$ is independent of the gauge-fixing vector.

3.3 Discussion: longitudinal fragmentation

We now consider the secondary quark contribution to longitudinal fragmentation in more detail. First, we compare the secondary quark contribution (see Fig. 3) with the corresponding contribution in the massive gluon scheme. The ratio

$$R(x) = \frac{A_{2,L}^{q,[s]} * D_q(x)}{A_{2,L}^{g,\text{MG}} * D_g(x)} \quad (62)$$

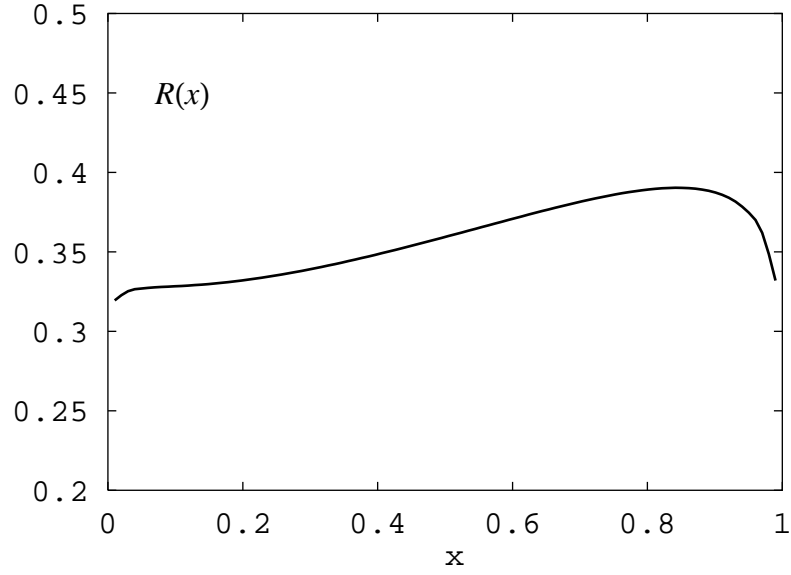


Figure 6: Ratio of secondary quark contribution in the fermion-loop approximation and gluon contribution in the massive gluon scheme.

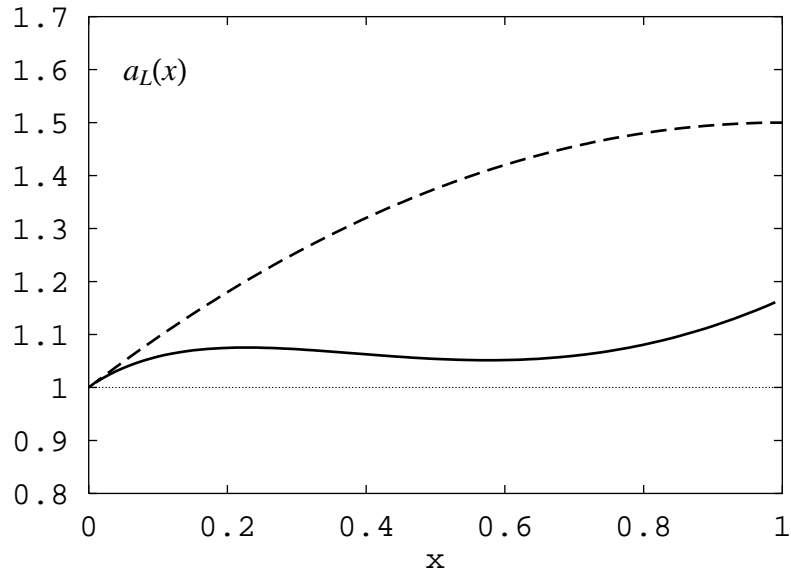


Figure 7: $a_L^q(x)$ (solid), $a_L^{sq}(x)$ (dashed) as defined in the text, compared with the massive gluon scheme (dotted).

is plotted in Fig. 6. Note that the fermion-loop approximation and massive gluon scheme coincide for the primary quark contribution, while the secondary quark contribution is smaller by a factor of about 3 than its massive gluon analogue. The difference in absolute normalization would be meaningful only if we tried to fix the constants K_2^i in terms of a single (universal) number as in [18]. If the K_2^i are considered as adjustable parameters as proposed here, the important message conveyed by Fig. 6 is that the ratio R is flat, so that the same x dependence is obtained with the two methods. The remaining variation is insignificant within the experimental uncertainties in the parametrization of leading-twist fragmentation functions and the theoretical uncertainties of our method.

Second, we compare the effective gluon coefficients obtained from secondary quarks and scalars as described above. The coefficients are given by⁵

$$A_{2,L}^{g\leftarrow q}(x) = \frac{72}{7x^3} + 18\frac{\ln x}{x} - \frac{15}{2x} - \frac{39}{14}\sqrt{x} \cos\left[\frac{\sqrt{7}}{2}\ln x\right] , \\ - \frac{3\sqrt{7}}{2}\sqrt{x} \sin\left[\frac{\sqrt{7}}{2}\ln x\right] \quad (63)$$

$$A_{2,L}^{g\leftarrow sq}(x) = \frac{8(1-x)}{x^3} (2 + 2x - x^2) , \quad (64)$$

for quarks and scalars, respectively. We recall that the gluon coefficient in the massive gluon scheme is simply $8(1-x)/x^3$, see (46). To compare the x dependence on a reasonable scale, we define

$$A_{2,L}^{g\leftarrow q}(x) = \frac{8(1-x)}{x^3} \cdot \frac{7}{8} \cdot a_L^q(x) , \quad (65)$$

$$A_{2,L}^{g\leftarrow sq}(x) = \frac{8(1-x)}{x^3} \cdot \frac{1}{2} \cdot a_L^{sq}(x) . \quad (66)$$

The normalizing factors are chosen such that $a_L(0) = 1$. The x dependence of a_L is shown in Fig. 7 for all three procedures (massive gluon, fermion or scalar loops). We observe again very little x dependence of the residual functions $a_L(x)$ and conclude that the method yields a unique result for $1/Q^2$ power corrections to longitudinal fragmentation. The residual different x dependence is definitely beyond any accuracy that can be expected from the model.

3.4 Discussion: transverse fragmentation

For the transverse fragmentation function, the effective gluon coefficients read

$$A_{2,T}^{g\leftarrow q}(x) = -18\frac{\ln x}{x} - \frac{51}{2x} + 12 + \frac{15}{2}\sqrt{x} \cos\left[\frac{\sqrt{7}}{2}\ln x\right] ,$$

⁵To compare absolute normalizations, the effective gluon coefficient obtained from quarks has to be divided by 3 and that obtained from scalars by 12 to take care of additional factors as in (41).

$$+ \frac{27}{2\sqrt{7}} \sqrt{x} \sin \left[\frac{\sqrt{7}}{2} \ln x \right] \quad (67)$$

$$A_{2,T}^{g \leftarrow sq}(x) = 0. \quad (68)$$

We have written the result for the transverse part separately, rather than the sum of transverse and longitudinal (referred to as ‘total’ in this subsection), in order to emphasize the absence of a $1/x^3$ term. Being absent for quarks and scalars, it follows that it is absent for gluon loops as well in any gauge; therefore, the statement is independent of how precisely the non-abelian contribution is reinstated. On the other hand, cancellation of the leading $1/x^3$ terms is most likely specific for the approximation of considering one chain of fermion bubbles and, in this sense, accidental as a peculiarity of the box graph. For $1/Q^4$ corrections, the leading term for small x , which is $1/x^5$ in this case, is indeed present for both transverse and longitudinal coefficients, see $A_{4,P}^{q,[s]}$ in Sect. 2.4.2. Since in large orders of perturbation theory diagrams with two chains of fermion loops are not suppressed, the cancellation that we observe does not imply, strictly speaking, any parametric suppression of the leading power correction for transverse fragmentation. A numerical suppression can hold, however, and it would be interesting to see whether it can be inferred from experimental data. Such a numerical suppression would be natural for the effective coupling approach of [12, 19].

Comparing these results with the massive gluon scheme, we observe that in this scheme the leading term $1/x^3$ at small x is cancelled in the sum of longitudinal and transverse coefficients, see (48). This cancellation appears to be unphysical and related to the fact that the structure of the massive gluon fragmentation cross section (43) is over-simplified. Indeed, the analytic terms in the ξ -expansion of (43) all behave as ξ^n/x^{2n+1} . On the other hand, non-analytic terms can arise only from the coefficient of the $\ln 1/(4\xi)$ -term, which does not have a non-trivial expansion in ξ . All terms $\xi^n \ln \xi$ vanish for $n > 3$ in this scheme, another indication that the massive gluon scheme may not capture the generic x dependence of power corrections in the case of total fragmentation functions.⁶

We compare the x dependence of the effective gluon coefficients obtained from quark and scalar loops for the total fragmentation cross section in Fig. 8. The relative normalization is chosen such that the asymptotic behaviours at small x coincide. Compared to Fig. 7, we have not scaled out the small- x behaviour, because we want to emphasize that the qualitative differences at large x will be insignificant for practical applications after convolution with the gluon fragmentation function, because primary quark fragmentation dominates in this region. Opposite to longitudinal fragmentation, the large- x behaviour of transverse secondary quark fragmentation is not unambiguously predicted by our model. While the scalar result vanishes linearly at $x = 1$, the quark result approaches a constant.

⁶We discuss in Sect. 4 that the presence of $1/(Q^2 x^2)^n$ power corrections for the total fragmentation function does not conflict with the absence of $1/Q$ power corrections to the integrated gluon fragmentation cross section.

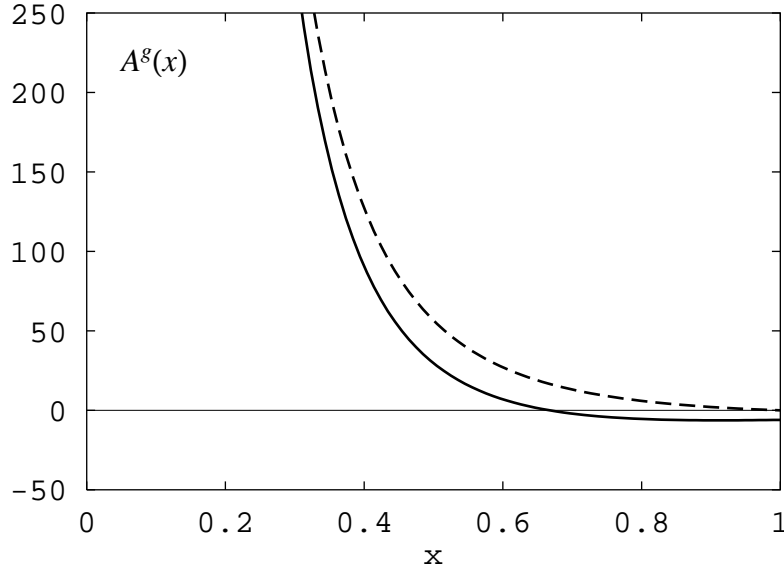


Figure 8: Comparison of effective gluon coefficients obtained from quarks (solid) and scalars (dashed) for the sum of longitudinal and transverse fragmentation.

Summarizing this discussion, we recommend the usage of the same functional form for the gluon coefficient in total fragmentation and in longitudinal fragmentation, but with a separate adjustable multiplicative constant (recall that for scalar quarks, in the present approximation, the two coefficients are in fact equal [Eqs. (58) and (60)], while for fermionic quarks they differ only slightly [Eqs. (37) and (39)]). If the adjustable constant for total fragmentation turns out to be close to the one for longitudinal fragmentation, it would indicate that the cancellation of $1/x^3$ terms for transverse fragmentation observed in our approximation is operative to a degree. If it turned out much smaller than for longitudinal fragmentation, this would provide support for the cancellation observed in the massive gluon scheme. In addition, we may add a constant to account for the $x \rightarrow 1$ behaviour. However, the value of this constant is not important in practice, unless it were abnormally large.

3.5 A simple parametrization

We summarize the analysis of this section in the form of a simple parametrization of $1/Q^2$ power corrections, which we suggest to apply to the analysis of fragmentation data. We write the fragmentation cross section (7) as

$$\frac{d\sigma_P}{dx}(x, Q^2) = \frac{d\sigma_P^{\text{LT}}}{dx}(x, Q^2) + \frac{d\sigma_P^{\text{power}}}{dx}(x, Q^2). \quad (69)$$

The leading-twist cross section is as in (2). The $1/Q^2$ power corrections are parametrized as

$$\begin{aligned} \frac{d\sigma_L^{\text{power}}}{dx}(x, Q^2) = & \frac{1\text{GeV}^2}{Q^2} \int_x^1 \frac{dz}{z} \left\{ c_{q,L} \left[\delta(1-z) + \frac{2}{z} \right] D_q(x/z, \mu) \right. \\ & \left. + c_{g,L} \frac{1-z}{z^3} D_g(x/z, \mu) \right\}, \end{aligned} \quad (70)$$

$$\begin{aligned} \frac{d\sigma_{L+T}^{\text{power}}}{dx}(x, Q^2) = & \frac{1\text{GeV}^2}{Q^2} \int_x^1 \frac{dz}{z} \left\{ c_{q,L+T} \left[-\frac{2}{[1-z]_+} + 1 + \frac{1}{2}\delta'(1-z) \right] D_q(x/z, \mu) \right. \\ & \left. + \left[c_{g,L+T} \frac{1-z}{z^3} + d \right] D_g(x/z, \mu) \right\}, \end{aligned} \quad (71)$$

where D_i denotes the leading-twist fragmentation function for parton i to decay into any given hadron, and the plus distribution is defined as usual,

$$\int_0^1 dx \frac{f(x)}{[1-x]_+} = \int_0^1 dx \frac{f(x) - f(1)}{1-x}, \quad (72)$$

for any test function f . The coefficients in front of quark fragmentation functions are taken from Sect. 2.4.1. The coefficients in front of gluon fragmentation functions follow from the discussion in Sects. 3.3 and 3.4. Note that for longitudinal fragmentation, we have neglected the residual x dependence displayed in Fig. 7 and chosen the simplest functional form. Let us add the following remarks:

(a) The overall scale $1\text{GeV}/Q$ (Q in GeV) has been chosen to set the overall magnitude for the constants c_k and d . With this scale, we expect these constants to be of order 1.

(b) The constants c_k and d should be fitted from the data. As mentioned above, the constant d is actually insignificant, so that the parametrization depends on four constants only. It is important that these constants should be quoted only in connection with a value for μ chosen for the factorization scale in the leading-twist contribution and also together with the order of perturbation theory to which the leading-twist coefficients C_P^i have been used. In this sense, the constants should be considered μ -dependent. We recall that the fermion-loop approximation considered in this paper suggests $c_{g,L} \simeq c_{g,L+T}$ while in the gluon mass scheme $c_{g,L} \gg c_{g,L+T}$.

(c) Since we did not consider additional logarithmic Q dependence of power corrections, the scale μ in D_i above is undetermined. Without additional information, it is natural to set μ equal to the scale used in the leading-twist part of the cross section.

(d) If the above parametrization of power corrections is used, no Monte Carlo correction for hadronization should be applied in addition.

(e) The ansatz can only be used as long as $x > \Lambda/Q$, where $\Lambda \sim 1\text{GeV}$ is a typical QCD scale. At smaller values of x , higher power corrections such as $1/Q^4$ become as

important as $1/Q^2$ corrections. In fact, the $1/Q^2$ expansion breaks down and would have to be resummed. In other words, (70) and (71) are corrections to the leading-twist prediction. If the power correction becomes as large as the leading-twist result, the ansatz fails.

4 $1/Q$ corrections to integrated cross sections

For $x > \Lambda/Q$ and not too close to 1, the power corrections discussed in the previous section arise only from regions of integration where two partons are collinear. In this section we consider moments of the x distributions, specifically the second moment (4), related to the integrated longitudinal and transverse cross sections, which are infrared finite.

The moments can have qualitatively different power corrections from those at finite x , because they include new infrared sensitive regions $x \rightarrow 0$ and $x \rightarrow 1$, related to soft partons. For small x this possibility is evident from the increasingly divergent terms $1/(Q^2 x^2)^n$ found in the secondary quark or gluon contributions. Thus, the integration over x must be performed before expansion in ξ . In other words, an infinite series of power corrections in $1/Q^{2n}$ has to be resummed to obtain the integrated cross section. Specifically, for the gluon contribution in the massive gluon scheme

$$\int_{\sqrt{\xi}} dx \frac{1}{2} x \frac{\xi^n}{x^{2n+1}} \sim \sqrt{\xi} \quad (73)$$

for any n . Recalling that ξ should be interpreted as Λ^2/Q^2 , we see that the small- x region can produce a $1/Q$ power correction, parametrically larger than at finite x .

In Sect. 4.1 we collect the distributions in ξ for the various contributions to the integrated cross section. Sect. 4.2 contains some observations on the relation of small- x behaviour and $1/Q$ corrections.

4.1 Longitudinal and transverse cross section

The primary quark contribution to the longitudinal and transverse cross sections is given by

$$\begin{aligned} \frac{\sigma_L^{q,[p]}}{\sigma_0} &= \frac{C_F \alpha_s}{2\pi} \cdot 2 \cdot \frac{1}{4} \left[(1 - \xi)(1 + 31\xi - 2\xi^2) + 12\xi \ln \xi + 6\xi^2(3 \ln \xi - \ln^2 \xi) \right] \\ &= \frac{C_F \alpha_s}{2\pi} \cdot 2 \cdot \left[\frac{1}{4} + \xi \left(3 \ln \xi + \frac{15}{2} \right) + \xi^2 \left(-\frac{3}{2} \ln^2 \xi + \frac{9}{2} \ln \xi - \frac{33}{4} \right) + \dots \right], \quad (74) \\ \frac{\sigma_T^{q,[p]}}{\sigma_0} &= \frac{C_F \alpha_s}{2\pi} \cdot 2 \cdot \left\{ \frac{2}{3} \ln \xi + \frac{22}{9} - 7\xi + \frac{17}{4} \xi^2 - \frac{22}{9} \xi^3 + \xi \ln \xi - \frac{9}{2} \xi^2 \ln \xi \right. \end{aligned}$$

$$\begin{aligned}
& + \frac{2}{3} \xi^3 \ln \xi - (1 + \xi)^2 \left[\ln \xi \ln(1 + \xi) - \frac{1}{2} \ln^2(1 + \xi) - \text{Li}_2\left(\frac{\xi}{1 + \xi}\right) \right] \Big\} \\
& = \frac{C_F \alpha_s}{2\pi} \cdot 2 \cdot \left[\frac{2}{3} \ln \xi + \frac{22}{9} - 6\xi + \xi^2 \left(\frac{3}{2} \ln^2 \xi - \frac{3}{2} \ln \xi + 6 \right) + \dots \right]. \quad (75)
\end{aligned}$$

The primary quark contribution does not contain odd powers of $\sqrt{\xi}$ and therefore no $1/Q$ power correction.

Because of large cancellations, it is again useful to present the distributions for the longitudinal and total secondary quark contribution. We have

$$\begin{aligned}
\frac{\sigma_L^{q,[s]}}{\sigma_0} &= \frac{(1 - \xi)(2 - 13\xi + 2\xi^2)}{4} - \frac{9\xi(1 + \xi)}{8} \ln \xi - \frac{15\xi(1 - \xi)}{32} \ln^2 \xi \\
&+ \left[\frac{15}{16}(1 + \xi^2) + \frac{27}{8}\xi \right] \sqrt{\xi} S(\sqrt{\xi}) \\
&= \frac{C_F \alpha_s}{2\pi} \left[1 - \frac{15\pi^3}{64} \sqrt{\xi} - 6\xi \ln \xi - \frac{27\pi^3}{32} \xi^{3/2} - \frac{46}{3} \xi^2 \ln \xi \right. \\
&\quad \left. + \frac{308}{9} \xi^2 - \frac{15\pi^3}{64} \xi^{5/2} + \dots \right], \quad (76)
\end{aligned}$$

where

$$\begin{aligned}
S(\lambda) &= -\frac{\pi^3}{8} + 2\lambda \int_0^1 \frac{\ln^2(\lambda t) dt}{1 + \lambda^2 t^2} = -\frac{\pi^3}{8} + i \ln^2 \lambda \ln \frac{1 - i\lambda}{1 + i\lambda} \\
&+ 2i [\ln \lambda (\text{Li}_2(i\lambda) - \text{Li}_2(-i\lambda)) - (\text{Li}_3(i\lambda) - \text{Li}_3(-i\lambda))] , \quad (77)
\end{aligned}$$

and no further half-integer powers of ξ appear in (76) beyond $\xi^{5/2}$. The total secondary quark contribution is simply

$$\frac{\sigma_{L+T}^{q,[s]}}{\sigma_0} = \frac{C_F \alpha_s}{2\pi} \left[-\frac{4}{3} \ln \xi - \frac{35}{9} - 6\xi \ln \xi - 3\xi - 6\xi^2 \ln \xi + 3\xi^2 - \frac{4}{3} \xi^3 \ln \xi + \frac{35}{9} \xi^3 \right]. \quad (78)$$

In the massive gluon scheme, the gluon contribution, to be compared with the secondary quark contribution, reads

$$\begin{aligned}
\frac{\sigma_L^{g,\text{GM}}}{\sigma_0} &= \frac{C_F \alpha_s}{2\pi} (1 + \xi) \left\{ 1 - \xi^2 + 2\xi \ln \xi + \xi \ln^2 \xi \right. \\
&- 4\sqrt{\xi} \left[(1 + \sqrt{\xi})^2 \left(\frac{1}{2} \ln \xi \ln(1 + \sqrt{\xi}) + \frac{\pi^2}{12} + \text{Li}_2(-\sqrt{\xi}) \right) \right. \\
&\quad \left. \left. + (1 - \sqrt{\xi})^2 \left(-\frac{1}{2} \ln \xi \ln(1 - \sqrt{\xi}) + \frac{\pi^2}{6} + \text{Li}_2(\sqrt{\xi}) \right) \right] \right\}
\end{aligned}$$

$$\begin{aligned}
&= \frac{C_F \alpha_s}{2\pi} \left[1 - \pi^2 \sqrt{\xi} + \xi \left(\ln^2 \xi - 2 \ln \xi + 9 + \frac{2\pi^2}{3} \right) - 2\pi^2 \xi^{3/2} \right. \\
&\quad \left. + \xi^2 \left(\ln^2 \xi - \frac{10}{3} \ln \xi + \frac{107}{9} + \frac{2\pi^2}{3} \right) + \dots \right], \tag{79}
\end{aligned}$$

$$\sigma_{L+T}^{g,\text{GM}} = \sigma_{L+T}^{q,[s]}. \tag{80}$$

Both the secondary quark contribution and the gluon contribution in the massive gluon scheme contain a $\sqrt{\xi}$ term, although with different coefficient. This term cancels in the sum of the longitudinal and transverse cross sections. Summing $\sigma_{tot} = \sigma_L^{q,[p]} + \sigma_T^{q,[p]} + \sigma_{L+T}^{q,[s]}$ we reproduce the distribution function for the total cross section given in Appendix B of Ref. [23]. Note that because the longitudinal and transverse cross sections are infrared finite, we continued to neglect explicit infrared factorization. However, the secondary quark contribution now contains the order- α_s gluon contribution.

4.2 Discussion

We now discuss some general aspects of how $1/Q$ corrections are generated in the gluon (secondary quark) contribution to the integrated cross section. As far as these general aspects are concerned, the fermion-loop approximation and the massive gluon scheme are the same and we choose the latter for the discussion, because the analytic expressions are simpler in this case.

We noted above, in Eq. (73), that $1/Q$ corrections are made possible, because the expansion parameter at finite but small x turned out to be ξ/x^2 rather than ξ . To obtain the coefficient of $\sqrt{\xi}$ in the integrated cross section, we need to pick up the most singular term in $1/x$ at every order in ξ . Once this is realized, the real question is not why $1/Q$ corrections arise in the integrated cross section, but why they do not arise in the sum of the longitudinal and transverse cross sections. Indeed, the most singular terms in the expansion of the total gluon cross section (43) are

$$\frac{1}{\sigma_0} \frac{d\sigma_{L+T}^{g,\text{MG}}}{dx} = \frac{C_F \alpha_s}{2\pi} \frac{4}{x} \left[\ln \frac{x^2}{\xi} - \sum_{n=1}^{\infty} \frac{(2n)!}{(n!)^2 n} \left(\frac{\xi}{x^2} \right)^n \right], \tag{81}$$

and the general structure of the expansion is the same as for the longitudinal and transverse cross sections separately. Integrating this expansion term by term, we obtain, for the coefficient a_1 of $\sqrt{\xi}$ in the expansion of $\sigma_{L+T}^{g,\text{MG}}$, the expression

$$a_1 = 4 \left[2(1 - \ln 2) - \sum_{n=1}^{\infty} \frac{(2n)!}{(n!)^2 n} \frac{2^{-2n}}{2n-1} \right]. \tag{82}$$

The sum is evaluated to

$$\sum_{n=1}^{\infty} \frac{(2n)!}{(n!)^2 n} \frac{2^{-2n}}{2n-1} = - \sum_{n=1}^{\infty} \frac{1}{n! n} \frac{\Gamma(n-1/2)}{\Gamma(-1/2)}$$

$$= \lim_{\epsilon \rightarrow 0} \frac{1}{\epsilon} [1 - {}_2F_1(-1/2, \epsilon, 1 + \epsilon; 1)] = 2(1 - \ln 2), \quad (83)$$

so that $a_1 = 0$, as is evident from (78). From this exercise we see that the cancellation of $1/Q$ corrections in the total gluon contribution is a property of the power expansion at fixed x only when all orders are included. Had we truncated the sum over n , a non-zero result would have been obtained. Furthermore, it is necessary to consider also analytic terms in the ξ expansion at fixed x to obtain the cancellation. This means that while $1/Q$ corrections are tied to soft partons, collinearity is not important.

We would like to note that these properties are reminiscent of those that lead to a cancellation of $1/Q$ corrections in the Drell-Yan cross section in the same (fermion-loop) approximation [26]. Contrary to the Drell-Yan process, however, we know for fragmentation that $1/Q$ corrections must cancel after summing over contributions from all partons, because the total e^+e^- annihilation cross section receives at most $1/Q^4$ power corrections (leaving aside issues related to parton-hadron duality). On the other hand, the cancellation of $1/Q$ terms in $\sigma_L^g + \sigma_T^g$ and $1/Q^2$ terms in $\sigma_{L+T}^g + \sigma_{L+T}^q$ looks rather accidental from the diagrammatic point of view.

The fact that the power expansion at fixed but small x runs in ξ/x^2 reminds us that the scale Λ of non-perturbative effects must be compared not with the total energy Q of the process, but with the energy $(Qx)/2$ of the detected hadron. To see this more transparently, consider the longitudinal gluon contribution (42). We may simplify the factor $(1 + \xi)(1 + \xi - x)$ to 1, because it does not alter $1/Q$ corrections, and we omit the factor $C_F \alpha_s / (2\pi)$. Now x times (42) depends on ξ and x only in the combination $x/\sqrt{\xi}$. The Borel transform $B[F]$ of the perturbative expansion generated by cut and virtual fermion-loop diagrams is related to the ξ distribution F by the Mellin transform [23]:

$$B[F](u, x) = -\frac{\sin \pi u}{\pi u} \int_0^1 d\xi \xi^{-u} \frac{d}{d\xi} F(\xi, x). \quad (84)$$

Because of the dependence on $x/\sqrt{\xi}$ only, the x dependence factorizes in the Borel transform as

$$B \left[\frac{1}{2} x \frac{d\sigma^{g, \text{MG}}}{\sigma_0 dx} \right] = \left(\frac{x}{2} \right)^{-2u} B(u), \quad (85)$$

with an x -independent function $B(u)$, which is easily obtained from (42) and (84). Its precise form will not be needed, but we note that $B(u)$ is analytic for $|u| < 1$ with a pole at $u = 1$ related to $1/Q^2$ power corrections. The (formal) Borel representation is now given by

$$\begin{aligned} \frac{1}{2} x \frac{d\sigma^{g, \text{MG}}}{\sigma_0 dx} &= \left(-\frac{1}{\beta_0} \right) \int_0^\infty du \exp \left(-\frac{u}{(-\beta_s \alpha_s(Q))} \right) \left(\frac{x}{2} \right)^{-2u} B(u) \\ &= \left(-\frac{1}{\beta_0} \right) \int_0^\infty du \exp \left(-\frac{u}{(-\beta_s \alpha_s(Qx/2))} \right) B(u). \end{aligned} \quad (86)$$

The x dependence is completely accounted for by setting the scale of the coupling constant to $Qx/2$, the energy of detected particles in the final state. Moreover, if we adhere to a strictly perturbative approach, the Borel integral diverges at infinity for $x < 2\Lambda/Q$ due to the Landau pole in the (one-loop) running coupling. Sensitivity to $u = \infty$ indicates that the entire power expansion in $1/Q^2$ needs to be resummed and that the renormalon approach is inapplicable at such small x .

Let us now define moments in x with a cut on x that eliminates the small- x region:

$$\sigma^{g,\text{MG}}(\gamma, x_c) \equiv \frac{1}{\sigma_0} \int_{x_c}^1 dx \frac{1}{2} x^{1+\gamma} \frac{d\sigma^{g,\text{MG}}}{dx}. \quad (87)$$

Eq. (85) gives

$$B[\sigma^{g,\text{MG}}(\gamma, x_c)](u) = \frac{1 - x_c^{1+\gamma-2u}}{1 + \gamma - 2u} 2 B(u). \quad (88)$$

Taking first $x_c = \gamma = 0$, we see that the $1/Q$ correction to the integrated longitudinal gluon cross section (corresponding to a pole of the Borel transform at $u = 1/2$) again is an immediate consequence of the scale being Qx . If the scale were $Q\sqrt{x}$, the denominator would read $1/(1-u)$ instead of $1/(1-2u)$.

Keeping $\gamma = 0$, we note that the pole at $u = 1/2$ is eliminated no matter how small x_c , as long as it is non-zero. Since in any experimental situation a minimum energy cut is required, the presence of $1/Q$ corrections in measured quantities depends on the value of x_c . If $x_c \sim \Lambda/Q$, the Borel transform is sharply peaked at $u = 1/2$ and the structure of large-order perturbation theory is indistinguishable from a $1/Q$ IR renormalon for practical purposes.

Taking $x_c = 0$, we note that the position of the pole depends on the moment. In particular, depending on γ , it is not bound to be integer or half-integer, a situation that never occurs in deep-inelastic scattering. It is this dependence on the precise weighting of long-distance regions (small x), first noted in [10], that makes $1/Q$ power corrections to σ_L and event shapes in general difficult to interpret in terms of operators (as in DIS) in the conventional sense. It also prompts some caution regarding the final conclusion on $1/Q$ corrections. It is conceivable that resummation of logarithmic terms $\ln^n x$ in perturbation theory modifies the approach to the small- x region. If, for illustration, resummation would turn x^{-2u} into $x^{\gamma-2u}$ in (85), a fractional power-correction would accordingly be obtained from (88). However, at present we do not know how to combine small- x resummation and constraints from angular ordering with a renormalon analysis.

The resummation of leading $\ln x$ can formally be achieved by a modification of the DGLAP evolution equation, which replaces the fragmentation functions $D_i(x/z, Q^2)$ with $D_i(x/z, x^2 Q^2)$ under the convolution integral [27]. The evolution equation then reads

$$Q^2 \frac{\partial}{\partial Q^2} D_g(N, Q^2) = \frac{\alpha_s(Q)}{2\pi} \int_0^1 dz z^{N-1} P_{g \rightarrow g}(z) D_g(N, z^2 Q^2). \quad (89)$$

Trading $\alpha_s(Q)$ for $1/(-\beta_0 \ln Q^2)$ and writing the fragmentation function formally as a

Mellin integral

$$D_g(N, Q^2) = \int_0^\infty du e^{-u/(-\beta_0\alpha_s(Q))} \tilde{D}(N, u) , \quad (90)$$

one can get the solution

$$\tilde{D}(N, u) \propto u^{-1-2\gamma_{gg}/b} (2u+1-N)^{2\gamma_{gg}/b} (2u-N)^{-4N_c/(Nb)} e^{1/b G(N, u)} , \quad (91)$$

where $\gamma_{gg} = 2N_c/(N-1)$, $b = -4\pi\beta_0$ and $G(N, u)$ is analytic at $N+1-2u > 0$. We approximated the gluon-gluon splitting function by its dominant term at small x . As $N \rightarrow 1$, the singularities at $u = 0$ and $u = (N-1)/2$ merge, and produce $\tilde{D}_g(N, u) \propto (1/u) \exp[-2N_c/(bu)]$, which gives rise to the correct small- x behaviour. On the other hand, (91) exhibits singularities at $u = (N-1+k)/2$, with $k = 1, 2, \dots$, which might indicate non-perturbative effects through power-suppressed ambiguities. Such an interpretation is, however, speculative, and we will not pursue it further in this paper. In general, one may ask, as for Drell-Yan production [25, 26], whether evolution equations of this type also give information on power corrections. In the above example, keeping only leading- $\ln x$ terms in each order of perturbation theory gives $2B(0)$ as residue of the pole at $u = 1/2$, while the correct result is $2B(1/2)$, see (88). In general, one has to be aware that systematic procedures to sum $\ln x$ terms may not work to power accuracy.

5 Perturbative corrections to σ_L and the determination of α_s

A measurement of the integrated longitudinal cross section could eventually yield a precise determination of the strong coupling. To approach this goal theoretically one has to control higher-order perturbative corrections, as well as non-perturbative effects, both of which are expected to be much larger for σ_L than for the total cross section σ_{tot} . In this section we consider perturbative corrections to σ_L , written as

$$\sigma_L = \sigma_0 \frac{\alpha_s}{\pi} \left[1 + \sum_{n=0}^{\infty} d_n (-\beta_0\alpha_s)^n \right] , \quad (92)$$

with $\beta_0 = -1/(4\pi)[11 - 2N_f/3]$ as before. We approximate the exact higher-order coefficient by its value in the ‘large- β_0 ’ limit, where β_0 is restored from the term with the largest power of N_f at each order. Given the ξ distributions for the primary and secondary quark contributions to σ_L in Sect. 4.1, the coefficients d_n are obtained numerically from the logarithmic moment integrals given in Eq. (12), as discussed in detail in [23]. The ‘large- β_0 ’ approximation, called ‘naive non-abelianization’ (NNA) in [23], reduces to the BLM scale setting prescription [28] for $n = 1$. To see how it works, we rewrite the exact α_s^2 correction in (5) as

$$d_1 = 6.17 - 0.7573/(-\beta_0). \quad (93)$$

n	$d_n^{q,[p]}(\overline{\text{MS}})$	$d_n^{q,[s]}(\overline{\text{MS}})$	$\sigma_{L,n}/\sigma_{tot}$	$d_n^{q,[s]}(V)$	$d_n^{sq,[s]}/d_n^{q,[s]}(V)$
0	1	1	0.036	1	1
1	11/2	13/2	0.052	29/6	1.121
2	29.82	45.97	0.060	27.07	1.203
3	164.1	369.0	0.064	188.8	1.226
4	944.1	3441	0.066	1634	1.219
5	5829	$3.734 \cdot 10^4$	0.068	$1.703 \cdot 10^4$	1.210
6	$3.940 \cdot 10^4$	$4.682 \cdot 10^5$	0.070	$2.088 \cdot 10^5$	1.205
7	$2.948 \cdot 10^5$	$6.707 \cdot 10^6$	0.071	$2.954 \cdot 10^6$	1.202
8	$2.447 \cdot 10^6$	$1.086 \cdot 10^8$	0.073	$4.751 \cdot 10^7$	1.201

Table 1: Perturbative corrections to σ_L as obtained from ‘naive non-abelianization’. The fourth column shows successive values for $\sigma_{L,n}/\sigma_{tot}$ at $Q = M_Z$ and with $\alpha_s(M_Z) = 0.118$. The last two columns show a comparison of NNA coefficients in the V scheme ($C = 0$) obtained from fermions or scalars. The asymptotic ratio of scalar and fermion coefficients is $6/5$; $\sigma_{tot}/\sigma_0 = 1.04$ has been used.

With $-\beta_0 = 0.61$ for $N_f = 5$, neglecting the second term gives an accuracy of about 25%. In particular, the approximation predicted correctly the large size of the second-order correction.

We have calculated the coefficients d_n in higher orders, in the $\overline{\text{MS}}$ scheme. The ‘primary’ and ‘secondary’ quark contributions, $d_n^{q,[p]}$ and $d_n^{q,[s]}$, respectively, add to d_n as $d_n = d_n^{q,[p]}/3 + 2d_n^{q,[s]}/3$. Columns 2 to 4 of Tab. 1 show the primary and secondary quark coefficients, together with successive finite-order approximations to σ_L/σ_{tot} based on these coefficients. The perturbative coefficients grow rapidly, especially for the secondary quark contribution. The fixed-sign growth and faster growth for the secondary quark contribution are directly related to an IR renormalon, indicating a $1/Q$ correction to secondary quark fragmentation as discussed in Sect. 4.

Since the longitudinal cross section is not fully inclusive with respect to gluon splitting into a quark-antiquark pair, restoration of the non-abelian piece is not unique, just as it was not unique for power corrections. The resulting ambiguity presents a major difficulty for the extension of ‘naive non-abelianization’ (and BLM scale setting) to hadronic event shape observables. We have not found a physically motivated modification of NNA that would alleviate this difficulty; therefore we investigated the ambiguity by comparing the higher-order coefficients obtained from restoring non-abelian contributions from both fermion and scalar loops.⁷ The comparison is shown in the last two columns of Tab. 1 in the V -scheme. To make a meaningful comparison in other schemes one would have to adjust the values of the strong coupling to take into account the difference between the

⁷This comparison was suggested to us by Lance Dixon.

finite parts of the fermion (scalar) loop. (In the $\overline{\text{MS}}$ scheme $C = -5/3$ for quarks and $C = -8/3$ for scalars.) It is seen that the ratio scalars/quarks is very stable around 1.2, which is the asymptotic limit in large orders and corresponds to the ratio of the coefficients of $\sqrt{\xi}$ in the expansion of the secondary quark distribution function. Consequently, the ambiguity in restoring the non-abelian contributions is at least 20%. However, in higher orders, the NNA prescription is probably less accurate than this anyway. The main point here is that radiative corrections to σ_L have the same sign and are consistently large already in low orders. Keeping this in mind, we conform to restoring higher-order contributions from fermion loops in the following.

The sum of $(\beta_0\alpha_s)^n$ contributions to all orders is conveniently written in terms of ‘enhancement factors’ [23], measured relative to the leading-order contribution. They are defined by

$$M^{[p,s]}(\alpha_s) = 1 + \sum_{n=0}^{\infty} (-\beta_0\alpha_s)^n d_n^{q,[p,s]}, \quad (94)$$

so that

$$\sigma_L^{(\text{NNA})} = \sigma_0 \frac{\alpha_s}{\pi} \left[\frac{1}{3} M^{[p]} + \frac{2}{3} M^{[s]} \right]. \quad (95)$$

In the following we define the sum to infinity in the sense of a principal value Borel integral, although truncating the series at its minimal term would be completely equivalent for practical purposes. For various values of $\alpha_s(M_Z)$ we get, at $Q = M_Z$,

$$\begin{aligned} \alpha_s = 0.110 : \quad & M^{[p]} = 1.59 \quad M^{[s]} = 1.92 \pm 0.05. \\ \alpha_s = 0.120 : \quad & M^{[p]} = 1.68 \quad M^{[s]} = 2.08 \pm 0.08. \\ \alpha_s = 0.130 : \quad & M^{[p]} = 1.79 \quad M^{[s]} = 2.23 \pm 0.12. \end{aligned} \quad (96)$$

The given uncertainties for the secondary quark contribution roughly coincide with the size of the minimal term in the series. The corresponding uncertainty for $M^{[p]}$ is small in comparison with the one for $M^{[s]}$ and is omitted. Interpolating between these values, one can get a rough idea of how $\sigma_L^{(\text{NNA})}$ changes with α_s .

Experience with similar calculations suggests that the approximation of resumming only $(\beta_0\alpha_s)^n$ contributions overestimates radiative corrections. A more realistic estimate would be expected to lie in between the resummed and the exact next-to-leading order (NLO) result. To see the magnitude of separate contributions, we take half of the Borel sum of $(\beta_0\alpha_s)^n$ contributions starting at order $n = 3$ to estimate the size of higher-order corrections. With $\alpha_s(M_Z) = 0.118$ we then get

$$\sigma_L/\sigma_{\text{tot}} = 0.0495 + (0.010 \pm 0.010) \pm 0.003, \quad (97)$$

where the first number corresponds to the NLO result, the second bracket presents our estimate of further perturbative corrections, and the third gives the estimated uncertainty in summation of the perturbation theory. At $Q = M_Z$ this uncertainty is rather moderate in size, even though it corresponds to a $1/Q$ correction. This suggests that although non-perturbative corrections to σ_L are much larger than to σ_{tot} , these corrections

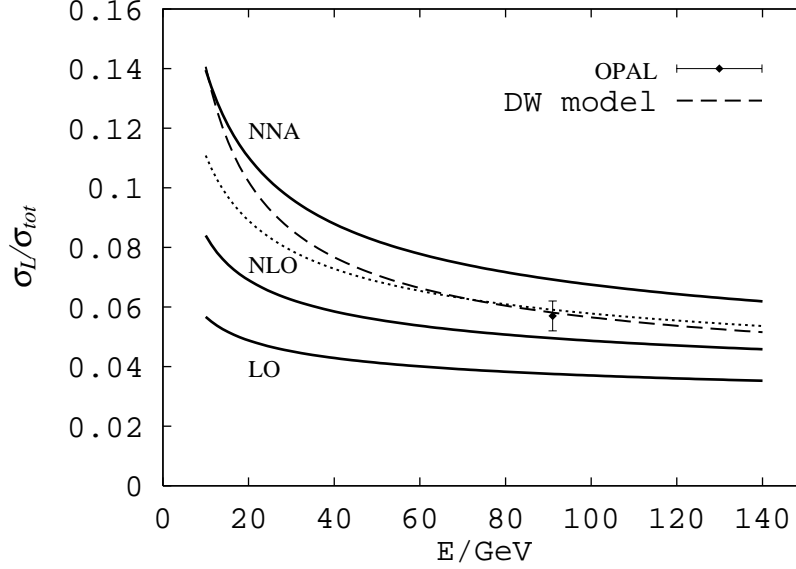


Figure 9: Longitudinal fraction in the total e^+e^- cross section calculated with $\alpha_s(M_Z) = 0.118$. Solid lines: leading order (LO), next-to-leading order (NLO) and resummation of all orders in $\beta_0^n \alpha_s^{n+1}$ corrected for the exact $O(\alpha_s^2)$ coefficient (NNA). Dashed line is the prediction of the Dokshitzer-Webber model and dotted line is the average of NLO and NNA calculations.

are still not large at $Q = M_Z$. An exact $O(\alpha_s^3)$ calculation would reduce the theoretical error considerably. Then, α_s determined from σ_L and σ_{tot} would provide an interesting consistency check.

Apart from measurements at a fixed energy, measuring the Q dependence of σ_L would be extremely interesting, especially at moderate energies. For other event shapes, it is known that a sizeable ‘hadronization correction’ must be added to second-order perturbation theory in order to reproduce the energy dependence. On the other hand, once higher-order corrections are computed, for example in an approximation such as ‘naive non-abelianization’, such hadronization corrections must be reconsidered, since the sum of higher-order corrections can already produce a steeper energy dependence.

To illustrate this point, we have plotted in Fig. 9 the energy dependence of the total longitudinal cross section, showing the leading-order (LO), next-to-leading order (NLO) and the resummed (NNA) results. We note the pronounced energy dependence of the resummed result towards lower energies. It is noteworthy that Monte Carlo parton showers do not produce such an energy dependence (see Fig. 5 of [2]) and resum a different set of higher-order corrections. At the same time, since higher-orders in $(\beta_0 \alpha_s)^n$ are inseparable from $1/Q$ power corrections, it is plausible that a substantial part of the conventional hadronization correction effectively parametrizes these higher-order corrections.

A similar conclusion can be drawn from a comparison of the resummed NNA re-

sult with the prediction obtained in the approach of Dokshitzer and Webber (DW) [12], compare the dotted and the dashed curves in Fig. 9. The Dokshitzer-Webber approach assumes universality of $1/Q$ power corrections and parametrizes them by an effective coupling. The dashed curve has been obtained following the prescription of [12] with the effective coupling fitted from the average $1 - T$ (T is thrust) and the relative coefficient of $1/Q$ for $1 - T$ and σ_L determined in the massive gluon scheme. In both cases the perturbative expansions are truncated at second order. It is seen that the energy dependence of the resummed perturbative results is not too different in NNA and the DW model. There is no conflict between the procedure of [12] and the resummation presented here, if the phenomenological $1/Q$ correction effectively parametrizes the higher-order perturbative contributions added in our approach. If universality of power corrections holds, these perturbative corrections would also be universal, at least asymptotically in large orders. However, from the point of view presented here, the universality assumption is not required, since higher-order corrections are in principle calculable for each observable.

6 Conclusions

In this paper we investigated power-suppressed corrections to fragmentation processes. Drawing on ideas derived from large-order perturbation theory and applied before with some success to deep-inelastic scattering [19, 20, 21], we have modelled the x dependence of the leading $1/Q^2$ power corrections. The method we use is consistent with the QCD light-cone expansion of Ref. [8] and can be considered as a model of the x dependence of certain twist-four correlation functions, based on the assumption of ‘ultraviolet dominance’ of higher-twist matrix elements. The theoretical status of this assumption, as discussed in Sect. 2, is rather dubious — eventually experimental results should clarify its relevance, as in the case of deep-inelastic scattering.

For the first time we were able to numerically analyse additional ambiguities that affect the method for observables where the hadronic final state is weighted or not fully inclusive. These additional ambiguities affect power corrections to event shapes in general [14] and also shed some light on the reliability of ‘massive gluon calculations’. In Sect. 3.5 we provided a parametrization of the x dependence of the leading ($1/Q^2$) power corrections, obtained by extracting the generic dependences on x from the comparison between different implementations of the method. The parametrization depends on four constants which, although of order unity, should be determined experimentally. We should mention that we did not address kinematic effects due to the finite mass of the final-state hadron, which should be treated separately, as is done for target-mass effects in deep-inelastic scattering.

From the theoretical point of view, fragmentation processes look like a promising place to pursue further outstanding questions related to the existence and interpretation of $1/Q$ power corrections in processes without operator product expansion, such as Drell-Yan production or event shapes. We have seen that the light-cone expansion breaks down

when $x \sim \Lambda/Q$ and quantities such as moments of the fragmentation cross section, which include the region of such small x , do not have a light-cone expansion. This situation is quite different from deep-inelastic scattering. In particular, the integrated longitudinal and transverse cross sections have a $1/Q$ correction. Fractional power corrections occur in fractional moments and in general the power behaviour of x -integrated quantities depends on the details of how the small- x region is weighted.

Acknowledgements. We are grateful to Bryan Webber for discussions and for informing us on [18] prior to publication. M. B. thanks Stan Brodsky and Lance Dixon for interesting discussions and the Institute for Nuclear Theory in Seattle for its hospitality while part of this work was done. V. B. is grateful to the Institute for Nuclear Theory in Seattle and the CERN Theory Group for their hospitality.

References

- [1] DELPHI collaboration, P. Abreu *et al.*, *Phys. Lett. B* **311** (1993) 408; contribution to ICHEP'96, Warsaw [pa01-022].
- [2] OPAL collaboration, R. Akers *et al.*, *Z. Phys. C* **68** (1995) 203.
- [3] ALEPH collaboration, D. Buskulic *et al.*, *Phys. Lett. B* **357** (1995) 487; *ibid.* **B 364** (1995) 247 (E).
- [4] P. Nason and B.R. Webber, *Nucl. Phys. B* **421** (1994) 473.
- [5] W. Furmanski and R. Petronzio, *Phys. Lett. B* **97** (1980) 437.
- [6] P.J. Rijken and W.L. van Neerven, *Phys. Lett. B* **386** (1996) 422, hep-ph/9604436; Leiden University preprints **INLO-PUB-09-96**, hep-ph/9609377 and **INLO-PUB-10-96**, hep-ph/9609379.
- [7] G.T. Bodwin, S.J. Brodsky and G.P. Lepage, *Phys. Rev. D* **39** (1989) 3287.
- [8] I.I. Balitsky and V.M. Braun, *Nucl. Phys. B* **361** (1991) 93.
- [9] H.D. Politzer, *Nucl. Phys. B* **172** (1980) 349; R.K. Ellis, W. Furmanski and R. Petronzio, *Nucl. Phys. B* **212** (1983) 29; R.L. Jaffe, *Nucl. Phys. B* **229** (1983) 205.
- [10] A.V Manohar and M.B. Wise, *Phys. Lett. B* **344** (1995) 407, hep-ph/9406392.
- [11] B.R. Webber, *Phys. Lett. B* **339** (1994) 148, hep-ph/9408222.
- [12] Yu.L. Dokshitser and B.R. Webber, *Phys. Lett. B* **352** (1995) 451, hep-ph/9504219.

- [13] R. Akhoury and V.I. Zakharov, *Phys. Lett. B* **357** (1995) 646, [hep-ph/9504248](#); *Nucl. Phys. B* **465** (1996) 295, [hep-ph/9507253](#); *Phys. Rev. Lett.* **76** (1996) 2238, [hep-ph/9512433](#).
- [14] P. Nason and M.H. Seymour, *Nucl. Phys. B* **454** (1995) 291, [hep-ph/9506317](#).
- [15] G.P. Korchemsky and G. Sterman, contribution to Moriond 1995: QCD and High Energy Hadronic Interactions [hep-ph/9505391](#).
- [16] Short reviews are given in M. Beneke, [hep-ph/9609215](#), to appear in the Proceedings of ICHEP'96, Warsaw; V.M. Braun, [hep-ph/9610212](#), to appear in the Proceedings of DPF'96, Minneapolis; R. Akhoury and V.I. Zakharov, [hep-ph/9610492](#), to appear in the Proceedings of QCD'96, Montpellier.
- [17] M. Beneke, V.M. Braun and L. Magnea, SLAC preprint **SLAC-PUB-7274**, [hep-ph/9609266](#), to appear in the Proceedings of QCD'96, Montpellier.
- [18] M. Dasgupta and B.R. Webber, Cavendish preprint **Cavendish-HEP-96/9**, [hep-ph/9608394](#), to appear in *Nucl. Phys. B*.
- [19] Yu.L. Dokshitzer, G. Marchesini and B.R. Webber, *Nucl. Phys. B* **469** (1996) 93, [hep-ph/9512336](#).
- [20] E. Stein *et al.*, *Phys. Lett. B* **376** (1996) 177, [hep-ph/9601356](#); M. Maul *et al.*, TU Munich preprint **TUM/T39-96-29**, [hep-ph/9612300](#).
- [21] M. Dasgupta and B.R. Webber, *Phys. Lett. B* **382** (1996) 273, [hep-ph/9604388](#).
- [22] M. Beneke, V.M. Braun and V.I. Zakharov, *Phys. Rev. Lett.* **73** (1994) 3058, [hep-ph/9405304](#).
- [23] M. Beneke and V.M. Braun, *Phys. Lett. B* **348** (1995) 513, [hep-ph/9411229](#); P. Ball, M. Beneke and V.M. Braun, *Nucl. Phys. B* **452** (1995) 563, [hep-ph/9502300](#).
- [24] M. Neubert, *Phys. Rev. D* **51** (1995) 5924, [hep-ph/9412265](#).
- [25] G.P. Korchemsky and G. Sterman, *Nucl. Phys. B* **437** (1995) 415, [hep-ph/9411211](#).
- [26] M. Beneke and V.M. Braun, *Nucl. Phys. B* **454** (1995) 253, [hep-ph/9506452](#).
- [27] B.R. Webber, Lectures at the Summer School on Hadronic Aspects of Collider Physics, Zuoz, 1994, [hep-ph/9411384](#).
- [28] S.J. Brodsky, G.P. Lepage and P.B. Mackenzie, *Phys. Rev. D* **28** (1983) 228.